

Charging Autonomous Electric Vehicle Fleet for Mobility-on-Demand Services: Plug in or Swap out?

Jing Gao, Sen Li

^a*Department of Civil and Environmental Engineering, The Hong Kong University of Science and Technology*

Abstract

This paper compares two prevalent charging strategies for electric vehicles, plug-in charging and battery swapping, to investigate which charging strategy is superior for electric autonomous mobility-on-demand (AMoD) systems. To this end, we use a queueing-theoretic model to characterize the vehicle waiting time at charging stations and battery swapping stations, respectively. The model is integrated into an economic analysis of the electric AMoD system operated by a transportation network company (TNC), where the incentives of passengers, the charging/operating shift of TNC vehicles, the operational decisions of the platform, and the planning decisions of the government are captured. Overall, a bi-level optimization framework is proposed for charging infrastructure planning of the electric AMoD system. Based on the proposed framework, we compare the socio-economic performance of plug-in charging and battery swapping, and investigate how this comparison depends on the evolving charging technologies (such as charging speed, battery capacity, and infrastructure cost). At the planning level, we find that when choosing plug-in charging, increased charging speed leads to a transformation of infrastructure from sparsely distributed large stations to densely distributed small stations, while enlarged battery capacity transforms the infrastructure from densely distributed small stations to sparsely distributed large stations. On the other hand, when choosing battery swapping, both increased charging speed and enlarged battery capacity will lead to a smaller number of battery swapping stations. At the operational level, we find that improved charging speed leads to increased TNC profit when choosing plug-in charging, whereas improved charging speed may lead to smaller TNC profit under battery swapping. The above insights are validated through realistic numerical studies.

Keywords: autonomous mobility-on-demand system, transportation network company, plug-in charging, battery swapping, charging infrastructure planning

1. Introduction

Automation, electrification, and shared mobility are dominating trends in developing an efficient and sustainable mobility future. Ride-hailing platforms, such as Uber, Lyft, Waymo and DiDi, are working at the forefront to realize this vision. For instance, Waymo has been providing autonomous rides in the East Valley of Phoenix since 2020 and is planning to expand its self-driving ride-hailing services to San Francisco in 2022 [1]. DiDi, as the world's largest shared electric vehicle (EV) network, has more than one million registered EVs, accounting for 20% of China's EV mileage [2]. With the advancement of autonomous driving and battery technologies, it is envisioned that shared autonomous electric vehicles (SAEVs) will be operated by Transportation Network Companies (TNC) to provide electric autonomous mobility-on-demand (AMoD) services in future cities. The economic and environmental benefits of electric AMoD services can

Email addresses: jgaoax@connect.ust.hk (Jing Gao), cesli@ust.hk (Sen Li)

be substantial. It is estimated that: (a) each 200-mile range SAEV could replace 5.5 privately owned cars under Level-2 charging [3]; (b) the cost of electric AMoD services will be \$0.29-\$0.61 per revenue mile [4], an order of magnitude lower than that of taxis; (c) the adoption of SAEVs can reduce greenhouse emissions by 73% and energy consumption by 58% [5].

Despite the aforementioned benefits, it remains unclear how to plan the charging infrastructure so that the charging needs of the commercial SAEV fleet can be most efficiently accommodated in future cities. There was a heat debate on whether we should prioritize plug-in charging or battery swapping for EVs. Each of the two charging strategies has its advantages and disadvantages. For instance, plug-in charging has a relatively low infrastructure cost, which can be conveniently installed and easily scaled up. However, typical Level-1 and Level-2 chargers require a few hours before charge completion, which incurs significant inconvenience for EV drivers. One way to overcome this limitation is by significantly accelerating the charging speed of EV batteries. As of today, the Tesla Supercharger can recharge up to 200 miles within 15 minutes [6], making it ideal for battery top-up in long-distance highway trips. Compared to fast-charging, an alternative approach is to swap the empty battery out of the EV and replace it with a fully-charged battery that is proactively stored in the battery swapping station. Battery swapping can eliminate the need for waiting, making it particularly popular among impatient customers: as one of the most successful Chinese EV companies, Nio has built over 900 battery swapping stations in 59 cities and executed more than 8 million battery swaps for its customers [7]. However, the major obstacle to the widespread adoption of battery swapping is that it requires standardization of batteries. This can be quite difficult because manufacturers can hardly agree on a uniform size of EV batteries. In addition, battery swapping also requires EV owners to widely accept the concept of battery-as-a-service, where the ownership of vehicles and batteries are separated so that EV drivers can willingly replace their empty batteries. Given these obstacles, many Western countries have chosen to primarily invest in fast-charging technologies instead of battery swapping stations.

So far, the comparison between plug-in charging and battery swapping is based on the assumption that most vehicles are human-driven and owned by individual drivers. However, with the advancement of self-driving technology, the landscape of urban mobility can be completely different in the future. In the autonomous-driving era, city residents may no longer owe his/her own car, which would otherwise sit at the parking garage for most of the time. Instead, autonomous vehicles will be shared, and the mobility needs of the city residents will be accommodated by electric AMoD services provided by TNC platforms. These changes in urban mobility have great potential to improve the efficiency of vehicle fleet utilization, lower the travel cost of passengers, and reduce energy consumption and carbon emissions from the transport sector. However, these changes also call for a re-investigation of how to choose the optimal charging strategies for future mobility systems with a large fleet of commercial SAEVs. In this case, the advantages and disadvantages of plug-in charging and battery swapping should be re-evaluated. On the one hand, while it is unarguable that fast charging still remains competitive for energy top-ups of long-distance highway trips, it is not necessarily a dominating charging option when considering large commercial SAEV fleets in the urban context. This is because the commercial SAEV fleet requires super fast charging as any downtime of vehicles in the commercial fleet cuts in the revenue. However, fast-charging infrastructure requires a much higher voltage and current (e.g., 200 A, 400 V) than its Level-1 (e.g., 12 A, 120 V) and Level-2 (e.g., 32 A, 240 V) alternatives [8]. In the urban context, building a large and densely distributed fast-charging network for SAEVs may incur significant voltage drops and cause instability to the already strained distribution power grids, which are prohibitively expensive to upgrade. On the other hand, battery swapping remains a competitive option for AMoD systems because the commercial SAEV fleet is owned by the TNC platform, thus it is much easier to enforce battery standardization by using the same type of vehicles, and there is no vehicle-battery ownership concerns when one battery is replaced with another. This naturally raises the following questions: (1) which charging strategy is superior for electric AMoD in the urban context, plug-in charging or battery swapping? (2) how does the comparison between plug-in charging and battery swapping depend on charging technologies, such as charging speed, battery capacity, and infrastructure

cost? (3) what is the optimal plan of charging infrastructure that maximizes social welfare?

This paper aims to address the aforementioned questions by comparing the performance of plug-in charging and battery swapping in AMoD systems from the socio-economic perspective. To this end, we need to carefully examine how commercial vehicles are queued up at charging stations/battery swapping stations, how the charging demand of the vehicles relates to the travel demand of the passengers, and how these relations are coordinated by the TNC platform and influenced by the government. A complete understanding of these complex relations requires the development of an equilibrium model, which captures the dynamics of charging stations and battery swapping stations while simultaneously encoding the intimate interactions between distinct stakeholders in the AMoD market. This paper will offer such a model, based on which we will investigate how different charging strategies (e.g., plug-in charging vs battery swapping) affect the planning decisions of the government, how they affect the operational decisions of the TNC platform, and how these impacts vary under different charging technologies (such as charging speed, battery capacity, infrastructure cost, etc). The major contributions of this paper are summarized below:

- We compare the socio-economic performance of plug-in charging and battery swapping for electric AMoD systems. To this end, we use a queueing-theoretic model to characterize the waiting time and the blocking probability at charging stations and battery swapping stations and integrate the model into an economic analysis of the AMoD market, where the incentives of passengers, TNC platforms, and the government are captured, and their interactions are characterized. Overall, a bi-level optimization framework is proposed for optimal planning of charging infrastructures. In the upper level, the government determines the infrastructure deployment plan to maximize social welfare. In the lower level, the TNC determines the fleet size and the ride fare to maximize its profit subject to market equilibrium constraints. *To our best knowledge, this is the first work that jointly considers the economics of the AMoD market, the planning decisions of the government, and the comparison between plug-in charging and battery swapping for the electric AMoD system.*
- We evaluate how the planning decisions of the government depend on the choice of charging strategies and the evolution of charging technologies. Based on our model, we find that when choosing plug-in charging, increased charging speed results in a transformation of charging deployment from *sparsely distributed large stations* to *densely distributed small stations*, while enlarged battery capacity transforms the infrastructure deployment from *densely distributed small stations* to *sparsely distributed large stations*. On the other hand, when choosing battery swapping, both increased charging speed and enlarged battery capacity lead to a smaller number of battery swapping stations. We identify the reason for this difference and show that the change in planning decisions for plug-in charging arises from the trade-off between the vehicle searching time before finding a charging station and the vehicle waiting time after arriving at the charging station.
- We evaluate how the operational decisions of the TNC platform depend on the choice of charging strategies and the evolution of charging technologies. We find that when choosing plug-in charging, improved charging speed leads to increased TNC profit. However, when choosing battery swapping, the TNC profit may reduce if the charging speed is relatively high. We point out that this can be attributed to the smaller degree of flexibility when deploying battery swapping stations compared to plug-in charging stations.

2. Related Works

This paper uses a queueing-theoretic model to characterize the vehicle waiting time at charging stations and battery swapping stations, which is further incorporated into the economic analysis and the charging infrastructure planning of the electric AMoD system. Thus, we review related works from the following

three perspectives: (1) queueing models for EV charging, (2) economic analysis of electric AMoD systems, and (3) charging infrastructure planning of electric AMoD systems.

2.1. Queueing models for EV charging

Queueing-theoretic models are extensively applied to characterize the vehicle charging process at charging stations. Some works characterize congestion at the charging stations and/or the equilibrium choices of the charging demand. For instance, [9] developed a queueing network model to estimate the charging demand of plug-in EVs, in which each charging station is modeled as a service center with multiple chargers as servers, and EVs are modeled as customers requesting charging services. [10] analyzed the performance of the EV platoons charging at renewable energy-supplied stations. The steady state of the queueing system was derived based on the equilibrium equations. [11] formulated a dual-mode charging station as a queueing network with multiple servers and heterogeneous service rates. The optimal pricing scheme is designed to guide the charging processes of EVs to minimize the service drop rate. [12] adopted the M/D/C queueing model to capture the congestion in charging stations and proposed an EV charging station access equilibrium model to characterize EV user equilibrium choices in charging stations. Aside from the aforementioned works, some other works also considered the impacts of charging stations on the power grid. For instance, [13] established an equilibrium queueing model to characterize the vehicle charging process that considers both the congestion in the distribution grid and the congestion due to the limited number of chargers/charging slots within charging stations. [14] considered the public charging stations with both grid-to-vehicle and vehicle-to-grid and developed an extended M/M/K/K queueing model to analyze the charging/discharging process at charging stations with K charge/discharge cord plugs.

Queueing models are also developed to characterize EV charging at battery swapping stations. The mechanisms of battery swapping station is more complicated than that of the charging stations. For instance, [15] proposed a mixed queueing network model to analyze the battery swapping station for electric vehicles, which is comprised of an open queue of EVs and a closed queue of batteries. The equilibrium equations of the queueing systems are formulated, and the steady-state distribution is derived. Based on the novel queueing network model, [16] formulated the charging operation problem of the battery swapping station as a constrained Markov decision process and derived the optimal charging policy that minimizes the charging cost while guaranteeing the quality of service. Likewise, based on the mixed queueing model, [17] conducted extensive simulations to evaluate the performance of the battery swapping station and charging station using the blocking probability of electric vehicles as the quality-of-service metric. Different parameters of the battery swapping and charging station are examined, such as the number of parking spaces, swapping islands, chargers, and batteries. [18] built a two-stage priority queueing model to capture the queueing effect of swapping and onboard charging processes. [19] introduced a closed Markovian queueing network model to represent the evolution of the battery population within a city and proposed a load-balancing policy to achieve the optimal trade-off between EV users' quality-of-service and operational costs.

Our paper differs from all aforementioned works as we integrate the queueing-theoretic model into the economic analysis of AMoD systems. In our paper, the main focus is on characterizing how the dynamics of the charging station and battery swapping station affect the incentives of passengers, platforms, and the social planner in the AMoD market. These elements are missing in the above-mentioned works.

2.2. Economic analysis of electric AMoD systems

A large body of works considered temporal dynamics and focused on the dynamic control of electric AMoD systems. Generally, they considered profit-maximizing AMoD operators and focused on the real-time charging scheduling [20, 21, 22, 23, 24, 25, 26], routing [20, 22, 23, 24], rebalancing [21, 25] and pricing [24, 25, 26, 27] of electric AMoD systems. For instance, [20] presented a model predictive control (MPC)

algorithm to optimize the vehicle scheduling and routing in the AMoD system with electric vehicle charging constraints. [21] investigated an online charge scheduling strategy for the electric AMoD system, in which autonomous electric vehicles are scheduled to charge between AMoD rides and dispatched to the next passenger pick-up locations. [22] optimized the routing, relocation, and charge scheduling of the SAEV fleet at two different time scales by running two MPC optimization algorithms in parallel. [23] considered the joint vehicle coordination and charge scheduling problem for electric AMoD systems where a mixed-integer linear program was presented to account for the battery level of vehicles and the energy availability in the power grid along the time horizon. [24] examined the joint routing, battery charging, and pricing problem for a profit-maximizing electric AMoD operator considering the randomness in trip demand, renewable energy availability, and electricity prices. [27] designed a pricing mechanism in a bi-level framework for the electric mobility-on-demand system to incentivize passengers to choose electric mobility-on-demand services. [25] proposed a combined operation scheme for the battery swapping station and AMoD system, where an expanded network flow model was developed to determine the dynamic swapping schedules and vehicle rebalancing for profit maximization of the AMoD system. [26] considered the interaction between the AMoD fleet and the battery swapping stations. A bi-level optimization problem was formulated to capture the interdependence between the AMoD system and the battery swapping system, wherein at the upper level, the battery swapping operator determines the time-varying and location-varying swapping price to minimize its cost, and at the lower level, the AMoD operator develops fleet scheduling strategies to maximize its profit.

Another strand of studies focused on the steady state and developed economic equilibrium models to investigate the implications of electric AMoD systems. For instance, [28] studied the potential benefits of smart charging for electric AMoD services, where a profit-maximizing operator makes decisions on routing, charging, rebalancing, and pricing for AMoD rides based on a network flow model. [29] studied the interaction between the AMoD system and the electric power network. A joint optimization model was proposed to capture vehicles' charging requirements, time-varying customer demand, battery depreciation, and power transmission constraints. It was proved that the socially optimal solution to the joint problem is a general equilibrium if locational marginal pricing is used for electricity. [30] investigated the impacts of competition in electric AMoD systems. A network-flow model was formulated to determine the optimal strategies for profit-maximizing electric AMoD operators in monopoly and duopoly markets. The benefits of introducing competition in the market were demonstrated by distinct metrics, including the prices of rides, aggregate demand served, profits of the firms, and consumer surplus. [31] investigated the problem of routing, rebalancing, and charging for electric AMoD systems concerning traffic congestion at the macroscopic level. A volume-delay function was introduced to characterize traffic congestion, and the routing and rebalancing for vehicles with energy constraints and charging constraints was formulated as an optimization problem.

However, all aforementioned studies considered the electric AMoD system under exogenous charging infrastructures, which neglects charging infrastructure planning and its impacts on the operation of electric AMoD systems. In addition, the majority of these work focused on charging stations, while only a few considered battery swapping. Distinct from these works, we characterize the interactions between the AMoD operator and the planner under both charging stations and battery swapping stations. This enables us to compare the two charging strategies in terms of both planning decisions and operational decisions, which have not been studied before in the aforementioned literature.

2.3. Charging infrastructure planning of electric AMoD systems

Numerous studies have investigated the planning of infrastructure for both charging stations [32, 33, 34, 35, 36, 37] and battery swapping stations [38, 39, 40, 41, 42]. However, most of these works focused on contemporary transportation systems, where the majority of vehicles are privately-owned and driven by individuals. On the other hand, only a handful of work considers the charging infrastructure planning for electric AMoD systems. For instance, [43] investigated the operation of SAEVs with charging infrastructure

development based on agent-based simulations. Different characteristics of SAEV fleets, including the fleet size, vehicle range, and charge time, were examined, and the simulation results indicated that the number of stations needed for the operation of SAEV fleets depends almost wholly on vehicle range. [44] explored the impacts of charging station placement, charging types, and vehicle battery capacity on the efficiency of SAEV services through agent-based simulations. Their results suggested that the performance of SAEV service can be significantly improved by offering battery swapping infrastructure. [45] proposed a framework to optimize charging infrastructure development for electric vehicle adoption in shared autonomous fleets. Several factors were considered, including the level of autonomous vehicle adoption, ridesharing participation, vehicle queueing at charging stations, and the tradeoff between building new charging stations and expanding existing ones. [46] considered the joint optimization of autonomous electric vehicle fleet operations and charging station siting. A linear program was introduced to jointly optimize the charging station siting and macroscopic fleet operations. They showed that small-sized EVs with low procurement costs and high energy efficiencies are the most cost-effective.

However, the aforementioned studies on AMoD [43, 44, 45, 46] primarily focus on plug-in charging (instead of battery swapping), and the majority of them [43, 44, 45] deploys agent-based simulation for given passenger demands, neglecting the incentive of passengers, which is a crucial aspect of the ride-hailing market. In contrast, our work differs from these studies as we consider the comparison between plug-in charging and battery swapping, the incentives of decision-makers in the electric AMoD market, and the planning decisions of the government.

3. Economic Equilibrium of the Electrified AMoD Market

Consider a TNC platform that operates a fleet of autonomous electric vehicles to provide AMoD services. The platform deploys a specific charging strategy and determines the ride fare and the fleet size to maximize its profit subject to the availability of charging infrastructure. In response to the platform’s pricing and charging strategy, passengers and the platform make interactive decisions, which constitute the market equilibrium. In this section, we develop an economic equilibrium model to characterize the ride-sourcing market equilibrium with electric autonomous vehicles. The incentives of passengers will be captured, and the dynamic charging process of vehicles will be characterized.

3.1. Passenger incentives

Passengers decide whether to choose AMoD services based on the total travel cost of the trip. We define the travel cost of AMoD as the weighted sum of *average* ride fare p_f and *average* waiting time w^c :

$$c = p_f + \alpha w^c, \tag{1}$$

where p_f is the average trip fare for the AMoD services, w^c is the average passenger waiting time before pick-up, and α is the value of time which indicates the passengers’ perception between time and money. We assume that the average passenger arrival rate λ depends on the generalized travel cost c and define the following passenger demand function:

$$\lambda = \lambda_0 F_p(p_f + \alpha w^c), \tag{2}$$

where λ_0 is the arrival rate of potential passengers (total travel demand in the city); $F_p(\cdot) \in [0, 1]$ determines the proportion of potential passengers choosing autonomous ride-hailing services. Note that (2) determines the passenger demand as a function of the average generalized cost, which does not require the cost of distinct travelers to be the same. We further assume that $F_p(\cdot)$ is a strictly decreasing and continuous

differentiable function such that a higher travel cost leads to a lower arrival rate of passengers. This includes the well-established logit model as a special case.

The passenger waiting time w^c represents the quality of electric AMoD services, which endogenously depends on the vehicle supply and passenger demand of the ride-hailing market. In ride-hailing services, the passenger waiting time comprises the ride confirmation time (from the ride request being submitted to a vehicle being assigned) and the pickup time (from a vehicle being assigned to passenger pickup). Typically, the ride confirmation time only lasts for several seconds, which is negligible compared to the pickup time ranging from five to eight minutes. Therefore, we neglect the ride confirmation time and approximate the passenger waiting time as the pickup time. Assuming that the platform matches the passenger to the nearest idle vehicle, the pickup time depends on the distance of the nearest idle vehicle to the passenger, which can be further characterized as a monotone function of the average number of idle vehicles N^I . We denote the passenger waiting time function as $w^c = F_c(N^I)$ and impose the following assumption:

Assumption 1. $F_c(N^I)$ is positive, strictly decreasing with respect to N^I , and $\lim_{N^I \rightarrow 0} F_c(N^I) = \infty$.

The passenger waiting time follows the "square root law", which was well-established and widely applied in street hailing taxi market [47], radio dispatching taxi market [48], and online ride-hailing market [49]. This leads to the following passenger waiting time function:

$$w^c = F_c(N^I) = \frac{A}{\sqrt{N^I}}, \quad (3)$$

where A is the scaling parameter capturing possible factors in the matching of idle vehicles and passengers, such as the area of the city, the average traffic speed on the road network, the spatial distribution of passengers/vehicles, etc. The square root law indicates that the average passenger waiting time is inversely proportional to the square root of the number of idle vehicles. The intuition behind (3) is that if both waiting passengers and idle vehicles are randomly distributed across the city, the distance between a passenger and her closest idle vehicle is inversely proportional to the square root of the total number of idle vehicles. A detailed justification of the square root law can be found in [50, 49].

3.2. The operating and charging shifts of TNC vehicles

TNC vehicles need to be charged due to the limited battery range. Once the platform decides that a vehicle needs to recharge, it will pause the AMoD services for the vehicle and dispatch it to nearby charging infrastructure for energy top-up (referred to as the "charging shift"). After being fully charged, it resumes to provide AMoD services (referred to as the "operating shift"). Throughout the day, each TNC vehicle regularly switches between the operating shift and the charging shift. On average, the total number of TNC vehicles (N) can be decomposed as the sum of two groups: vehicles in the operating shift (N_1) and vehicles in the charging shift (N_2). This leads to the following relation:

$$N = N_1 + N_2. \quad (4)$$

The characterization of N_1 , N_2 , and their endogenous relations will be discussed below.

3.2.1. The operating shift

During the operating shift, autonomous electric vehicles provide ride-hailing services to passengers, in which vehicles experience the following three statuses sequentially and recurrently: (1) status 1: being idle and cruising for passengers; (2) status 2: being assigned with passengers and picking up passengers; (3) status 3:

being occupied with passengers and delivering passengers. Let τ be the average duration of the ride-hailing trips. At the stationary state, the conservation of the total vehicle operating hour yields:

$$N_1 = N^I + \lambda w^c + \lambda \tau, \quad (5)$$

where the first term corresponds to the average number of idle vehicles in the operating shift (status 1), and the second term and third term are derived based on Little's law, which represents the average number of vehicles on the way to pick up passengers (status 2), and the average number of vehicles delivering passengers (status 3), respectively. Let w^v be the average vehicle idle time between rides, i.e., the average duration of status 1. Based on Little's law, the number of idle vehicles N^I relates to w^v through the following equation:

$$N^I = \lambda w^v \quad (6)$$

At the stationary state, the number of vehicles in operating shifts (N_1) and the number of vehicles in charging shifts (N_2) endogenously depend on the charging process of autonomous electric vehicles. Next, we focus on the charging shift of TNC vehicles and derive the relations of N_1 , N_2 , and other endogenous variables.

3.2.2. The charging shift

During the charging shift, vehicles are dispatched to nearby charging infrastructures (either charging stations or battery swapping stations) for battery top-up. There may be matching frictions between vehicles and charging infrastructure, so that each vehicle may have to spend some time traveling to the charging infrastructure. Furthermore, upon arrival at the charging infrastructure, each vehicle may also need to wait until a charging device is available for immediate use. Overall, the charging process of autonomous electric TNC vehicles can be divided into three phases: (1) phase 1: searching for nearby charging/battery swapping stations; (2) phase 2: waiting for charging at charging/battery swapping stations; (3) phase 3: being charged at charging/battery swapping stations. Let N_2^m , N_2^w , and N_2^s be the average number of vehicles in the three phases, and denote t_m , t_w , and t_s as the average duration of the three phases, respectively. At the stationary state, the conservation of the total number of vehicles in charging shifts yields:

$$N_2 = N_2^m + N_2^w + N_2^s. \quad (7)$$

Besides, based on Little's law, we have the following relations:

$$\begin{cases} N_2^m = \gamma t_m \\ N_2^w = \gamma t_w \\ N_2^s = \gamma t_s \end{cases}, \quad (8)$$

where γ is the arrival rate of vehicles in charging shifts, which is an endogenous variable representing the charging demand of autonomous electric TNC vehicles. Below we derive the relations among these endogenous variables separately.

To derive t_m , we assume that arriving vehicles in the charging shift are dispatched to the nearest charging/battery swapping station that is not full for battery replenishment. Due to the limited capacity, the charging/battery swapping station may be full and have no idle parking spaces for vehicles waiting. In this case, the average vehicle searching time equals the average travel time between the vehicle and the nearest charging/battery swapping station with vacant parking spaces. Let V be the average capacity of each charging/battery swapping station and denote P_V as the probability of a station being full. The average vehicle searching time t_m is inversely proportional to the square root of the number of charging/battery swapping stations that are not full [51, 52, 53]:

$$t_m = \frac{B}{\sqrt{K(1 - P_V)}}, \quad (9)$$

where B is the scaling parameter, K is the number of charging/battery swapping stations, and $K(1 - P_V)$ accounts for the number of charging/battery swapping stations that are not full. It follows the same intuition as the derivation of (3): if both vehicles and charging/battery swapping stations are randomly distributed across the city, the expected distance between a vehicle to the closet available charging/battery swapping station is inversely proportional to the square root of the number of available charging/battery swapping stations. Note that the blocking probability P_V is an endogenous variable that depends on both the charging demand γ and the configuration of charging/battery swapping stations.

To derive P_V , t_w , and t_s , we note that they have different relations with other endogenous variables under different charging strategies (i.e., plug-in charging v.s. battery swapping). To reflect these differences, we will characterize the operating mechanism of charging stations and battery swapping stations separately.

Queueing Model for Plug-in Charging: We use an M/M/Q/V queue model to represent the vehicle charging process at each charging station as shown in Figure 1a. Consider a fleet of autonomous electric vehicles with a battery capacity of C , which will be dispatched to nearby available charging stations once the battery SoC approaches the minimum SoC. In practice, the platform determines vehicles' charging schedules based on vehicles' real-time operating statuses. Therefore, vehicles arriving at charging/battery swapping stations may have distinct SoCs and different charging times. Without loss of generality, let δ be the mean battery SoC of vehicles arriving at charging/battery swapping stations¹. Suppose that there are K charging stations uniformly distributed across the city, and each station has the capacity V and Q chargers with charging speed s (see Figure 1b the schematic of Tesla's charging station). Each charger can be modeled as a server, and arrived vehicles can be regarded as jobs. A charger is 'busy' if it is occupied by a vehicle. Otherwise, it is considered as 'idle'. We assume that the arrival of TNC vehicles at each charging station follows the Poisson process. The total charging demand of TNC vehicles is γ , and thus the arrival rate of vehicles at each station is γ/K . Furthermore, since each vehicle in the charging shift will be charged to full, the average vehicle charging time (service time) is $t_s = (1 - \delta)C/s$. If we further assume that the vehicle charging times (service times) are exponentially distributed, then the vehicle charging process at each charging station can be modeled as an M/M/Q/V queue with arrival rate γ/K and service rate $1/t_s$. Define the system state as the number of vehicles in the charging station and denote $\rho = \frac{\gamma t_s}{K}$ and $a = \frac{\gamma t_s}{KQ}$. The steady-state distribution of the M/M/Q/V queueing system is given by [54]:

$$P_v = \begin{cases} \frac{\rho^v}{v!} P_0, & \text{if } 0 \leq v \leq Q \\ \frac{\rho^v}{Q^{v-Q} Q!} P_0, & \text{if } Q \leq v \leq V \end{cases} \quad (10)$$

where $P_0 = \left(\sum_{v=0}^{Q-1} \frac{\rho^v}{v!} + \sum_{v=Q}^V \frac{\rho^v}{Q^{v-Q} Q!} \right)^{-1}$ is the probability of the system having no vehicles, and P_v is the probability of the system holding v vehicles (including those in service). Given the steady-state distribution (10), the blocking probability P_V and the average vehicle waiting time t_w can be characterized as [54]:

$$P_V = \frac{\rho^V}{Q^{V-Q} Q!} \left(\sum_{v=0}^{Q-1} \frac{\rho^v}{v!} + \sum_{v=Q}^V \frac{\rho^v}{Q^{v-Q} Q!} \right)^{-1}, \quad (11)$$

and

$$t_w = \frac{a \rho^Q [1 - a^{V-Q+1} - (1-a)(V-Q+1)a^{V-Q}] K}{\gamma(1-a)^2(1-P_V)Q!} \left(\sum_{v=0}^{Q-1} \frac{\rho^v}{v!} + \sum_{v=Q}^V \frac{\rho^v}{Q^{v-Q} Q!} \right)^{-1} \quad (12)$$

Equation (11) and (12) capture the blocking probability P_V and the average vehicle waiting time t_w as a function of the charging demand γ , the number of charging stations K , the number of chargers at each

¹The mean battery SoC should depends on the charging schedules of the platform, which we regard as exogenous.

station Q , the capacity of the station V , the battery capacity C , and the charging speed s , respectively. This corresponds to the practice that the vehicle waiting time for charging depends on both the demand, the infrastructure supply, and the battery/charging technologies.

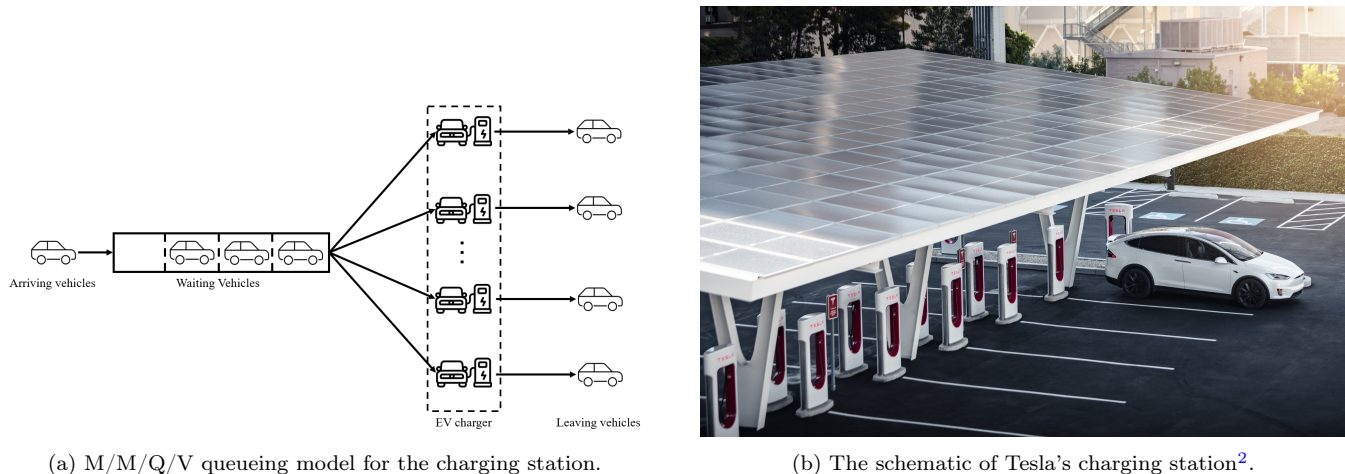


Figure 1: M/M/Q/V model for the charging station and Tesla's charging station.

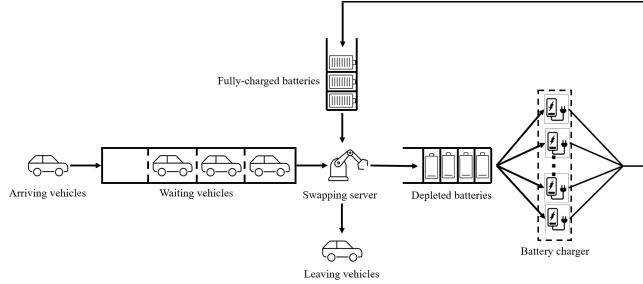
Queueing Model for Battery Swapping: Compared to plug-in charging, battery swapping has a more complicated operating mechanism since it involves not only battery swapping for electric vehicles but also charging for batteries inside the swapping station. These two processes occur simultaneously and interact with each other. On the one hand, arrived vehicles can only start service when there are fully-charged batteries and unoccupied swapping servers/robots. Otherwise, they have to wait for services, which produces an open queue of electric vehicles. On the other hand, each depleted battery will swap another fully-charged battery out, which implies that there is a closed queue/circulation of batteries inside the station. The strong coupling of the open queue and the closed queue makes it difficult to apply conventional queueing models (e.g., M/M/N queue) to characterize such a system. Inspired by [15], we use a mixed queueing network to model the battery swapping station³. Below we detail the mixed queueing network model.

Consider a fleet of electric TNC vehicles with a battery capacity of C . There are K battery swapping stations uniformly distributed over the city. The battery swapping station is modeled as a mixed queueing network which consists of an open queue of EVs and a closed queue of EV batteries, as shown in Figure 2a. Let us take Nio's battery swap station as the prototype (see Figure 2b the schematic of Nio's battery swap station). Each swapping station has a single server (i.e., robot/machine) that can execute battery swapping for the customer and Q chargers that can replenish energy for depleted batteries. Batteries swapped out of the vehicles are stored and immediately recharged by the battery chargers. For simplicity, we assume that the number of stored batteries per station is identical to the number of chargers at each station, i.e., Q . Due to limited parking spaces, it is assumed that a maximum number of V vehicles can wait for battery swapping services. Therefore, the open queue of the EVs in the mixed queueing network has a capacity/buffer size of V . We further assume that the two buffers in the closed queue of EV batteries are large enough to hold all the batteries. Therefore, there will be no deadlock and blocking in the closed queue [55]. The battery swapping server/robot has a constant service time t_s (e.g., 2 minutes) for each battery swapping service, which accounts for the time needed for exchanging batteries. We define the system state

²Retrieved 2023, from <https://www.tesla.com/supercharger>. Copyright 2023 by Tesla. Reprinted with permission.

³The mixed queueing model is similar to the model proposed in [15]. However, different from [15], we primarily focus on characterizing the average vehicle waiting time t_w and integrating it into the economic analysis of the AMoD systems.

of the battery swapping station⁴ at any time t as $S_t = (v_t, q_t)$, where $v_t \in [0, V]$ denotes the number of TNC vehicles present in the station, and $q_t \in [0, Q]$ represents the number of fully-charged batteries in the closed queue. Let $\mathcal{S} = \{(v, q) | v \in [0, V], q \in [0, Q]\}$ be the state space. Now we derive the steady-state distribution of the queueing network to characterize the average vehicle waiting time at battery swapping stations.



(a) The queueing network model for the battery swapping station.



(b) The schematic of Nio's battery swap station⁵.

Figure 2: The mixed queueing model for the battery swapping station and Nio's battery swap station.

We first characterize vehicle arrivals at the queueing network. For any given time t , we consider the time interval $(t, t + t_s]$. Let $g(v)$ be the probability of v new vehicle arrivals at the battery swapping station during $(t, t + t_s]$. Assuming that the arrival process of autonomous electric TNC vehicles at each battery swapping station is Poisson with rate γ/K ⁶, then the probability $g(v)$ can be written as:

$$g(v) = \frac{e^{-\gamma t_s/K} (\gamma t_s/K)^v}{v!} \quad v \geq 0, \quad (13)$$

which is derived based on the probability density function of Poisson distribution with mean arrival $\gamma t_s/K$.

Next, we consider the dynamic of the closed queue of batteries. Let $f(m, n)$ be the probability of n batteries finishing charging by time $t + t_s$ given that there are m batteries being charged at time t . Analogous to vehicle charging service, we assume that battery charging times of different chargers follow independent and identical exponential distributions. Once the battery level approaches the minimum SoC, TNC vehicles go to nearby battery swapping stations to swap depleted batteries with fully-charged batteries. Similarly, let δ be the average battery SoC of vehicles that arrive at battery swapping stations. The corresponding average battery charging time is $t_c = (1 - \delta)C/s$. In this case, $f(m, n)$ can be considered as the probability of getting n batteries fully charged within $(t, t + t_s]$ in $\min\{Q, m\}$ independent Bernoulli trials with success probability $1 - e^{-t_s/t_c}$. Therefore, $f(m, n)$ is given by the probability mass function of the binomial distribution:

$$f(m, n) = \binom{\min\{Q, m\}}{n} \left(1 - e^{-t_s/t_c}\right)^n e^{-t_s/t_c (\min\{Q, m\} - n)}, \quad (14)$$

where $n \in [0, \min\{Q, m\}]$, indicating that the number of batteries finishing charging by $(t, t + t_s]$ is bounded above by the number of batteries being charged at time t and the total number of chargers.

Given (13) and (14), we can further establish the dynamics of the queueing system. Without loss of generality, let $S_t = (v_t, q_t)$ be the state of the system at time t holding v_t electric vehicles and q_t fully-charged batteries, and let $S_{t+t_s} = (v_{t+t_s}, q_{t+t_s})$ be the system state at time $t + t_s$ with v_{t+t_s} electric

⁴The state is defined for a single battery swapping station and we focus on its steady-state equilibrium. By assuming that the demand is uniformly distributed to distinct stations, we do not need to distinguish one battery swapping station to another.

⁵Retrieved 2022, from <https://www.nio.com/nio-power>. Copyright 2022 by NIO. Reprinted with permission.

⁶The total charging demand of TNC vehicles is γ , so the arrival rate of vehicles at each battery swapping station is γ/K .

vehicles and q_{t+t_s} fully-charged batteries. Denote $P_t(v_t, q_t) = \Pr(S_t = (v_t, q_t))$ and $P_{t+t_s}(v_{t+t_s}, q_{t+t_s}) = \Pr(S_{t+t_s} = (v_{t+t_s}, q_{t+t_s}))$ as the corresponding probability of the system state $S_t = (v_t, q_t)$ and $S_{t+t_s} = (v_{t+t_s}, q_{t+t_s})$, respectively. Based on the Bayes' law, the state probability at time $t + t_s$ can be written as:

$$P_{t+t_s}(S_{t+t_s}) = \sum_{S_t \in \mathcal{S}} P_t(S_t) \cdot \Pr(S_{t+t_s}|S_t), \quad (15)$$

where \mathcal{S} is the state space, and the conditional probability $\Pr(S_{t+t_s}|S_t)$ represents the transition probability from state S_t to S_{t+t_s} . To characterize this transition probability, we note that the service time is t_s , and thus the vehicle in service at time t will have left the system by time $t + t_s$, and the swapped depleted battery will have started charging at time $t + t_s$. In this regard, all vehicles present at time $t + t_s$ either arrived within $(t, t + t_s]$ or were already waiting for service at time t . In addition, all fully-charged batteries present at time $t + t_s$ were either charged during $(t, t + t_s]$ or already fully charged before t . Consequently, the transition probability from state $S_t = (v_t, q_t)$ to state $S_{t+t_s} = (v_{t+t_s}, q_{t+t_s})$ is given by:

$$\begin{aligned} & \Pr(S_{t+t_s} = (v_{t+t_s}, q_{t+t_s})|S_t = (v_t, q_t)) \\ &= \begin{cases} g(v_{t+t_s} - v_t + \min\{v_t, q_t, 1\}) \cdot f(Q - q_t, q_{t+t_s} - q_t + \min\{v_t, q_t, 1\}) & v_{t+t_s} \in [0, V - 1], q_{t+t_s} \in [0, Q] \\ \left(1 - \sum_{v=0}^{V-1} g(v - v_t + \min\{v_t, q_t, 1\})\right) \cdot f(Q - q_t, q_{t+t_s} - q_t + \min\{v_t, q_t, 1\}) & v_{t+t_s} = V, q_{t+t_s} \in [0, Q]. \end{cases} \end{aligned} \quad (16)$$

The intuition behind (16) is straightforward. The term $\min\{v_t, q_t, 1\}$ represents the count of vehicles that finished the battery swapping service within the time interval $(t, t + t_s]$. This count is limited by the number of vehicles v_t , the number of fully-charged batteries q_t at time t , and the number of swapping servers. Given that each battery swapping station has only one swapping server, either 0 or 1 vehicle will finish the battery swapping service and leave the station during $(t, t + t_s]$, depending on the presence of vehicles and the availability of batteries. Since there are v_t and v_{t+t_s} vehicles in the station at time t and $t + t_s$ respectively, and $\min\{v_t, q_t, 1\}$ vehicles have left the station during $(t + t_s]$, when $0 \leq v_{t+t_s} \leq V - 1$, the number of vehicle arrivals within $(t, t + t_s]$ is $v_{t+t_s} - v_t + \min\{v_t, q_t, 1\}$. The corresponding probability is $g(v_{t+t_s} - v_t + \min\{v_t, q_t, 1\})$ according to (13). Due to the limited capacity V , all cases with new vehicle arrivals not less than $V - 1 - v_t + \min\{v_t, q_t, 1\}$ make state $S_t = (v_t, q_t)$ transit to state $S_{t+t_s} = (V, q_{t+t_s})$. Therefore, the probability of new vehicle arrivals during $(t, t + t_s]$ when $v_{t+t_s} = V$ is given by $1 - \sum_{v=0}^{V-1} g(v - v_t + \min\{v_t, q_t, 1\})$. Furthermore, since there are q_t and q_{t+t_s} fully-charged batteries at time t and $t + t_s$ respectively, and $\min\{v_t, q_t, 1\}$ fully-charged batteries have been swapped out during $(t, t_s]$, the number of batteries being charged at time t is $Q - q_t$, and the number of batteries finished charging during $(t, t + t_s]$ is $q_{t+t_s} - q_t + \min\{v_t, q_t, 1\}$. According to (14), the probability of battery charging is $f(Q - q_t, q_{t+t_s} - q_t + \min\{v_t, q_t, 1\})$. Finally, the product of vehicle arrival probability and battery charging probability gives the state transition probability (16).

Next, we derive the steady-state distribution of the mixed queueing network to represent the long-run equilibrium status of the battery swapping station. Denote $P(v, q) = \lim_{t \rightarrow \infty} P_t(v_t, q_t)$ as the steady-state probability of the station holding v vehicles and q fully-charged batteries. Plugging (16) into (15), the steady-state equations can be written as:

$$P(v, q) = \begin{cases} \sum_{\hat{v}=0}^V \sum_{\hat{q}=0}^Q P(\hat{v}, \hat{q}) \cdot g(v - \hat{v} + \min\{\hat{v}, \hat{q}, 1\}) \cdot f(Q - \hat{q}, \hat{q} - q + \min\{\hat{v}, \hat{q}, 1\}) & v \in [0, V - 1] \\ \sum_{\hat{v}=0}^V \sum_{\hat{q}=0}^Q P(\hat{v}, \hat{q}) \cdot \left(1 - \sum_{u=0}^{V-1} g(u - \hat{v} + \min\{\hat{v}, \hat{q}, 1\})\right) \cdot f(Q - \hat{q}, \hat{q} - q + \min\{\hat{v}, \hat{q}, 1\}) & v = V \end{cases}. \quad (17)$$

Equation(s) (17) form a finite system of $(V + 1)(Q + 1)$ linear equations. The solution to (17) together with the normalization equation $\sum_{v=0}^V \sum_{q=0}^Q P(v, q) = 1$ gives the steady-state distribution of the battery swapping system.

Finally, based on the steady-state distribution, we derive the blocking probability P_V and the average vehicle waiting time t_w at battery swapping stations. Given $P(v, q)$, the blocking probability P_V of the queueing system, i.e., the probability of the swapping station being full, can be determined as:

$$P_V = \sum_{q=0}^Q P(V, q). \quad (18)$$

The average number of vehicles at each battery swapping station is given by:

$$\bar{N} = \sum_{v=0}^V \sum_{q=0}^Q vP(v, q). \quad (19)$$

Further, based on Little's law, the average number of vehicles at each station \bar{N} can also be written as:

$$\bar{N} = \frac{\gamma}{K} (1 - P_V) (t_w + t_s), \quad (20)$$

where γ/K represents the average arrival rate of vehicles at each station, t_w is the average vehicle waiting time at battery swapping stations, and t_s is the constant service time. Combining equations (19) and (20) derives the average waiting time t_w as:

$$t_w = \frac{K \sum_{v=0}^V \sum_{q=0}^Q vP(v, q)}{\gamma(1 - P_V)} - t_s. \quad (21)$$

Remark 1. *We assume that the charging time follows the exponential distribution with mean charging time $(1 - \delta)C/s$ when deriving the queueing model for both plug-in charging and battery swapping. While the exponential distribution may not fully characterize the exact distribution of vehicles' charging times (should be a truncated distribution, where the truncation occurs at the minimum SoC incurred by the platform), we argue that the independent and identical exponential distributions of charging times capture (i) the average charging time that stems from the platform's charging scheduling and (ii) the independence between different chargers and batteries, which are fundamental aspects of the queueing system. This assumption offers mathematical tractability, and is widely used in EV charging-related literature [15, 53, 56, 57] to serve as reasonable approximations and facilitate the derivation of the analytical model.*

3.3. The balance of energy

At the stationary state, the electricity consumed by the autonomous electric vehicle fleet and the electricity charged to the fleet should be balanced regardless of the charging strategies adopted by the TNC platform. Let l be the average hourly electricity consuming rate of autonomous electric TNC vehicles, and then we have the following energy balance equation:

$$(N - N_2^w - N_2^s)l = \gamma(1 - \delta)C, \quad (22)$$

where γ is the charging demand of TNC vehicles, N_2^w is the number of TNC vehicles waiting at charging stations (or battery swapping stations), and N_2^s is the number of vehicles being charged at the charging station (or serviced at the battery swapping station). The term $N - N_2^w - N_2^s$ accounts for the average number of TNC vehicles traveling on roads, and the left-hand side of (22) represents the hourly electricity consumption by those vehicles cruising on the street. In per-unit time, γ vehicles arrive at charging/battery stations with the average battery level δC and leave with full battery capacity C , and thus the electricity input to the system per hour is $\gamma(1 - \delta)C$. The consumed and charged electricity should be balanced at the stationary equilibrium.

4. Charging Infrastructure Planning: Bilevel Optimization Model

In this section, we consider the profit maximization decision of the TNC platform and its interaction with the government, which deploys electric vehicle charging infrastructures to promote social welfare. Overall, the problem can be formulated with a bilevel optimization framework: on the upper level, the government designs the infrastructure deployment plan for social welfare maximization; at the lower level, the TNC determines the operational strategy for profit maximization. This section mathematically formulates the bilevel optimization model. The platform's strategic decisions for profit maximization and the government's infrastructure deployment for social welfare maximization will be introduced separately.

4.1. Profit maximization for the TNC

The revenue of the TNC platform is the ride fares collected from passengers, and the cost consists of two parts: (1) electricity cost; and (2) investment and operating cost of the fleet. Let p_e be the average electricity price and let C_{av} be the average hourly operating cost of a TNC vehicle. In each hour, the platform collects λp_f ride fares from passengers, spends $\gamma(1 - \delta)C p_e$ electricity costs for charging vehicles and NC_{av} operating costs for the autonomous vehicle fleet. The difference between the revenue and the cost is the platform profit. Given the upper-level government's deployment of charging infrastructures (either charging stations or battery swapping stations), the TNC determines the ride fare and the fleet size to maximize its profit subject to the market equilibrium constraints. The TNC's profit-maximization problem under the strategy of plug-in charging and battery swapping can be formulated as follows, respectively.

- TNC's profit maximization under plug-in charging

$$\max_{p_f, N} \quad \lambda p_f - \gamma(1 - \delta)C p_e - NC_{av} \quad (23)$$

$$\left\{ \begin{array}{l} \lambda = \lambda_0 F_p(p_f + \alpha w^c) \end{array} \right. \quad (24a)$$

$$\left\{ \begin{array}{l} w^c = \frac{A}{\sqrt{\lambda w^v}} \end{array} \right. \quad (24b)$$

$$\left\{ \begin{array}{l} \lambda(w^v + w^c + \tau) = N_1 \end{array} \right. \quad (24c)$$

$$\left\{ \begin{array}{l} N_1 + N_2 = N \end{array} \right. \quad (24d)$$

$$\left\{ \begin{array}{l} N_2^m + N_2^w + N_2^s = N_2 \end{array} \right. \quad (24e)$$

$$\left\{ \begin{array}{l} N_2^m = \gamma t_m \end{array} \right. \quad (24f)$$

$$\left\{ \begin{array}{l} N_2^w = \gamma t_w \end{array} \right. \quad (24g)$$

$$\left\{ \begin{array}{l} N_2^s = \gamma t_s \end{array} \right. \quad (24h)$$

$$\left\{ \begin{array}{l} t_m = \frac{B}{\sqrt{K(1 - P_V)}} \end{array} \right. \quad (24i)$$

$$\left\{ \begin{array}{l} P_V = \frac{\rho^V}{Q^{V-Q} Q!} \left(\sum_{v=0}^{Q-1} \frac{\rho^v}{v!} + \sum_{v=Q}^V \frac{\rho^v}{Q^{v-Q} Q!} \right)^{-1} \end{array} \right. \quad (24j)$$

$$\left\{ \begin{array}{l} t_w = \frac{a \rho^Q [1 - a^{V-Q+1} - (1-a)(V-Q+1)a^{V-Q}] K}{\gamma(1-a)^2(1-P_V)Q!} \left(\sum_{v=0}^{Q-1} \frac{\rho^v}{v!} + \sum_{v=Q}^V \frac{\rho^v}{Q^{v-Q} Q!} \right)^{-1} \end{array} \right. \quad (24k)$$

$$\left\{ \begin{array}{l} (N - N_2^w - N_2^s)l = \gamma(1 - \delta)C \end{array} \right. \quad (24l)$$

where $t_s = (1 - \delta)C/s$ accounts for the average vehicle charge/service time at charging stations, $\rho = \gamma t_s / K$ and $a = \gamma t_s / KQ$ are auxiliary variables, K represents the number of charging stations, Q denotes the number of chargers per station, V is the capacity of the charging station.

- TNC's profit maximization under battery swapping

$$\max_{p_f, N} \quad \lambda p_f - \gamma(1 - \delta)Cp_e - NC_{av} \quad (25)$$

$$\left\{ \begin{array}{l} \lambda = \lambda_0 F_p(p_f + \alpha w^c) \end{array} \right. \quad (26a)$$

$$\left\{ \begin{array}{l} w^c = \frac{A}{\sqrt{\lambda w^v}} \end{array} \right. \quad (26b)$$

$$\left\{ \begin{array}{l} \lambda(w^v + w^c + \tau) = N_1 \end{array} \right. \quad (26c)$$

$$\left\{ \begin{array}{l} N_1 + N_2 = N \end{array} \right. \quad (26d)$$

$$\left\{ \begin{array}{l} N_2^m + N_2^w + N_2^s = N_2 \end{array} \right. \quad (26e)$$

$$\left\{ \begin{array}{l} N_2^m = \gamma t_m \end{array} \right. \quad (26f)$$

$$\left\{ \begin{array}{l} N_2^w = \gamma t_w \end{array} \right. \quad (26g)$$

$$\left\{ \begin{array}{l} N_2^s = \gamma t_s \end{array} \right. \quad (26h)$$

$$\left\{ \begin{array}{l} t_m = \frac{B}{\sqrt{K(1 - P_V)}} \end{array} \right. \quad (26i)$$

$$\left\{ \begin{array}{l} P_V = \sum_{q=0}^Q P(V, q) \end{array} \right. \quad (26j)$$

$$\left\{ \begin{array}{l} t_w = \frac{K \sum_{v=0}^V \sum_{q=0}^Q v P(v, q)}{\gamma(1 - P_V)} - t_s \end{array} \right. \quad (26k)$$

$$\left\{ \begin{array}{l} (N - N_2^w - N_2^s)l = \gamma(1 - \delta)C \end{array} \right. \quad (26l)$$

where t_s denotes the average vehicle charge/service time at battery swapping stations, K is the number of battery swapping stations, Q is the number of chargers/batteries per station, V is the capacity of the battery swapping station, $P(v, q)$ is the steady-state distribution of the battery swapping station which can be derived from (17).

In the optimization (23) and (25), p_f and N are decision variables corresponding to the platform's pricing and fleet sizing strategy; λ , w^c , w^v , N_1 , N_2 , N_2^m , N_2^w , N_2^s , γ , t_m , t_w and P_V are involved endogenous variables; λ_0 , α , τ , δ , s , t_s , l , p_e , A , B , C , C_{av} , K , Q and V are model parameters. Note that there are a few differences between the market equilibrium models for plug-in charging (24) and battery swapping (26). For plug-in charging, the blocking probability P_V (24j) and the vehicle waiting time (24k) are derived based on the M/M/Q/V queue, whereas for battery swapping, the blocking probability P_V (26j) and the vehicle waiting time (26k) are derived from the mixed queueing model. In addition, the average vehicle charging/service time at charging stations t_s is associated with the charging speed and the battery capacity through $t_s = (1 - \delta)C/s$. However, the vehicle service time at battery swapping stations is considered as a constant, which is relatively short. These differences result from the fundamental operating mechanisms of charging stations and battery swapping stations.

4.2. Social welfare maximization for the government

On the upper level, the government deploys charging infrastructures in the city for social welfare maximization. In the ride-sourcing market with autonomous electric vehicles, the social welfare comprises the passengers' surplus, the profit of the TNC, and the cost of constructing and operating charging infrastructures. Let ϕ be the per charger investment and operating cost of a charging/battery swapping station in

each hour⁷. We define social welfare as the difference between the social benefit and the infrastructure cost:

$$\Pi_{SW} = \lambda_0 \int_c^\infty F_p(x)dx + \lambda p_f - \gamma(1 - \delta)Cp_e - NC_{av} - \phi KQ, \quad (27)$$

where c denotes the average travel cost of passengers, the term $\lambda_0 \int_c^\infty F_p(x)dx$ calculates the passengers' surplus, the term $\lambda p_f - \gamma(1 - \delta)Cp_e - NC_{av}$ represents the TNC profit, and the last term ϕKQ accounts for the total cost of charging facilities. The government designs the infrastructure deployment scheme to maximize social welfare. In particular, when planning charging stations for vehicle charging, the government determines the number of charging stations K and the number of chargers Q at each station to promote social welfare. Denote ϕ_{vc} as the per charger infrastructure cost of charging stations. The social welfare maximization for the government when planning charging stations can be formulated as the following bi-level optimization:

$$\begin{aligned} \max_{K>0, Q>0} \quad & \lambda_0 \int_c^\infty F_p(x)dx + \lambda p_f - \gamma(1 - \delta)Cp_e - NC_{av} - \phi_{vc}KQ, \\ \text{subject to} \quad & (23), (24a)-(24l). \end{aligned} \quad (28)$$

On the other hand, due to the closed structure and technological feasibility, battery swapping stations are usually standardized, and the number of chargers/batteries Q inside the swapping station is pre-designed by the manufacturer for ease of mass production (see the schematic of Nio's battery swap station in Figure 2b). Therefore, when deploying battery swapping stations, the government can only control the total number of battery swapping stations K to maximize social welfare. Let ϕ_{bs} be the per charger infrastructure cost of battery swapping stations. The social welfare maximization for the government when deploying battery swapping stations can be cast as:

$$\begin{aligned} \max_{K>0} \quad & \lambda_0 \int_c^\infty F_p(x)dx + \lambda p_f - \gamma(1 - \delta)Cp_e - NC_{av} - \phi_{bs}KQ, \\ \text{subject to} \quad & (25), (26a)-(26l). \end{aligned} \quad (29)$$

Remark 2. *In practice, different charging stations may have a distinct number of chargers considering the need for parking spaces and the spatial demand at different locations. This paper neglects these aspects and considers K uniformly distributed homogeneous charging stations with the same number of chargers at the aggregate level. We emphasize that such an aggregate model is sufficient for our purpose since we focus on revealing the interactions among different stakeholders (e.g., passengers, the TNC, and the government) in the electric AMoD market and the long-term charging infrastructure planning at the city level. The spatial imbalance of charging demand can be considered by extending our current model into a network equilibrium model, which is left for future work.*

4.3. Solution properties

The optimization (23) and (28), and the optimization (25) and (29) constitute the bilevel optimization framework for the government's infrastructure planning of charging stations and battery swapping stations, respectively. To justify the existence of the market equilibrium and solve the optimization, we first introduce the following three lemmas:

Lemma 1. *Given A and τ , in equilibrium (24) and (26), if $N_1 \geq \left(\sqrt[3]{2} + \sqrt[3]{\frac{1}{4}}\right) (A\lambda)^{\frac{2}{3}} + \lambda\tau$, there exist strictly positive w^c and w^v satisfying (24b)-(24c). Furthermore, w^c can be uniquely determined as a function of λ and γ from (24b)-(24c), i.e., $w^c = w^c(\lambda, N_1)$.*

⁷Note that the infrastructure cost is pro-rated. In addition, the cost parameter ϕ for charging and battery swapping stations may be distinct. Their difference will be reflected in the case study.

The proof of Lemma 1 can be found in Appendix B in our previous work [58]. The condition $N_1 \geq \left(\sqrt[3]{2} + \sqrt[3]{\frac{1}{4}}\right) (A\lambda)^{\frac{2}{3}} + \lambda\tau$ guarantees the existence of strictly positive w^c and w^v in equilibrium (24) and (26). Besides, $w^c = w^c(\lambda, N_1)$ can be uniformly derived under different charging strategies.

Lemma 2. *Given $\delta, s, t_s, l, B, C, K, Q$ and V , (i) in equilibrium (24), P_V, N_1 and N can be uniquely determined as a function of γ from (24d)-(24l), denoted as $\hat{P}_V(\gamma), \hat{N}_1(\gamma)$ and $\hat{N}(\gamma)$, where $\hat{N}_1(\gamma) = \frac{\gamma(1-\delta)C}{l} - \frac{\gamma B}{\sqrt{K(1-\hat{P}_V(\gamma))}}$; (ii) in equilibrium (26), P_V, N_1 and N can be uniquely determined as a function of γ from (26d)-(26l), denoted as $\tilde{P}_V(\gamma), \tilde{N}_1(\gamma)$ and $\tilde{N}(\gamma)$, where $\tilde{N}_1(\gamma) = \frac{\gamma(1-\delta)C}{l} - \frac{\gamma B}{\sqrt{K(1-\tilde{P}_V(\gamma))}}$.*

The proof of Lemma 2 can be found in Appendix A. It states that in equilibrium, given the exogenous model parameters and the upper-level infrastructure deployment plan, the blocking probability P_V , the number of operating vehicles N_1 , and the total fleet size N unilaterally depend on the charging demand γ . Furthermore, we have the following results on the property of $\hat{N}_1(\gamma)$ and $\tilde{N}_1(\gamma)$.

Lemma 3. *Given $\delta, s, t_s, l, B, C, K, Q$ and V , if $K > \left(\frac{Bl}{(1-\delta)C}\right)^2$, (i) there exist a unique $\hat{\gamma}_0 > 0$ and $\hat{\gamma}_* \in (0, \hat{\gamma}_0)$ such that $\hat{N}_1(\hat{\gamma}_0) = 0$, and $\forall \gamma \in (0, \hat{\gamma}_0)$, $0 < \hat{N}_1(\gamma) \leq \hat{N}_1(\hat{\gamma}_*)$; (ii) there exist a unique $\tilde{\gamma}_0 > 0$ and $\tilde{\gamma}_* \in (0, \tilde{\gamma}_0)$ such that $\tilde{N}_1(\tilde{\gamma}_0) = 0$, and $\forall \gamma \in (0, \tilde{\gamma}_0)$, $0 < \tilde{N}_1(\gamma) \leq \tilde{N}_1(\tilde{\gamma}_*)$.*

The proof of Lemma 3 can be found in Appendix B. It states that under two distinct charging strategies, when the number of charging/swapping stations is higher than $\left(\frac{Bl}{(1-\delta)C}\right)^2$, there exists a positive charging demand γ_0 at which the number of operating vehicles becomes zero. Furthermore, for any charging demand below γ_0 , there will be a positive number of operating vehicles N_1 , and the maximum number of operating vehicles is achieved at a $\gamma_* \in (0, \gamma_0)$. Without loss of generality, let $\hat{N}_1^{\max} = \hat{N}_1(\hat{\gamma}_*)$ and $\tilde{N}_1^{\max} = \tilde{N}_1(\tilde{\gamma}_*)$ be the maximum number of operating vehicles under plug-in charging and battery swapping, respectively. Based on the results of Lemma 1-3, we can justify the existence of the market equilibrium (24) and (26):

Proposition 1. *Given $\lambda_0, \alpha, \tau, \delta, s, t_s, l, A, B, C, K, Q$ and V , (i) if $K > \left(\frac{Bl}{(1-\delta)C}\right)^2$ and $F_p \left(\frac{\alpha A}{\sqrt{\hat{N}_1^{\max}}}\right) > 0$, there exist strictly positive $p_f, w^c, w^v, \lambda, \gamma, t_m, t_w, P_V, N, N_1, N_2, N_2^m, N_2^w$ and N_2^s that constitute a market equilibrium satisfying (24); (ii) if $K > \left(\frac{Bl}{(1-\delta)C}\right)^2$ and $F_p \left(\frac{\alpha A}{\sqrt{\tilde{N}_1^{\max}}}\right) > 0$, there exist strictly positive $p_f, w^c, w^v, \lambda, \gamma, t_m, t_w, P_V, N, N_1, N_2, N_2^m, N_2^w$ and N_2^s that constitute a market equilibrium satisfying (26).*

The proof of Proposition 1 is deferred to Appendix C. Both (i) and (ii) in Proposition (1) state the existence of the market equilibrium under distinct conditions. To guarantee the existence of the market equilibrium (24) and (26), Proposition 1 states that the supply of charging/battery swapping stations should exceed $\left(\frac{Bl}{(1-\delta)C}\right)^2$. Besides, the conditions $F_p \left(\frac{\alpha A}{\sqrt{\hat{N}_1^{\max}}}\right) > 0$ and $F_p \left(\frac{\alpha A}{\sqrt{\tilde{N}_1^{\max}}}\right) > 0$ indicate that when the TNC platform sets the ride fare p_f to 0 and has \hat{N}_1^{\max} and \tilde{N}_1^{\max} vehicles in operating under plug-in charging and battery swapping respectively, there will be a positive number of passengers. Overall, these are mild conditions that can be satisfied in reality.

The market equilibrium (24) and (26) involve a bunch of nonlinear constraints, e.g., (24k) and (26k), which makes the optimization problems (23) and (25) non-convex. Besides, due to the complex relations among the endogenous variables and the bi-level structure of the optimization, it is non-trivial to derive the partial derivatives and apply gradient-based algorithms to solve the bi-level optimization. However, since both (23) and (25) are small-scale problems with only two decision variables and several equality constraints, we can equivalently treat λ and γ as decision variables, absorb all the equality constraints into the objective function, and transform the profit maximization problem into an unconstrained optimization:

Lemma 4. Given the market equilibrium (24), (23) is equivalent to the following unconstrained optimization:

$$\max_{\lambda, \gamma} \quad \tilde{\Pi}_P(\lambda, \gamma) = \lambda \left[F_p^{-1} \left(\frac{\lambda}{\lambda_0} \right) - \alpha w^c \left(\lambda, \hat{N}_1(\gamma) \right) \right] - \gamma(1 - \delta)Cp_e - \hat{N}(\gamma)C_{av} \quad (30)$$

Lemma 5. Given the market equilibrium (26), (25) is equivalent to the following unconstrained optimization:

$$\max_{\lambda, \gamma} \quad \tilde{\Pi}_P(\lambda, \gamma) = \lambda \left[F_p^{-1} \left(\frac{\lambda}{\lambda_0} \right) - \alpha w^c \left(\lambda, \tilde{N}_1(\gamma) \right) \right] - \gamma(1 - \delta)Cp_e - \tilde{N}(\gamma)C_{av} \quad (31)$$

Lemma 4 and 5 derive the platform profit as a function of λ and γ under the strategy of charging vehicles and swapping batteries, respectively. By such transformations, for each charging infrastructure plan (K, Q) , we can apply the grid search to maximize (30) and (31), which provides the globally optimal solutions to the lower-level profit maximization problems (23) and (25). After solving the lower-level optimization, we can substitute the optimal solution into (27) to compute the corresponding social welfare produced by the infrastructure deployment scheme (K, Q) . Finally, we apply a grid search over all possible K and Q to find the optimal infrastructure deployment plan that maximizes the social welfare⁸.

5. Case Studies

This section investigates how the evolvement of charging technologies affects the charging infrastructure planning for the AMoD system. First, we calibrate the model parameters based on real-world TNC data. Second, we present case studies to investigate the impacts of charging speed and battery capacity. Lastly, we compare the TNC market outcomes under two distinct charging strategies.

5.1. Model parameters

Consider a case study for New York City. Assume passengers decide whether to choose AMoD services based on a logit model:

$$\lambda = \lambda_0 \frac{\exp(-\epsilon c)}{\exp(-\epsilon c) + \exp(-\epsilon c_0)}, \quad (32)$$

where c is the average generalized travel cost of ride-hailing trips; $\epsilon > 0$ and c_0 are model parameters. Besides, the blocking probability (24j) and the average waiting time (24k) involve summation and factorial, which restricts the number of chargers per station Q to be integers. For mathematical tractability, we apply analytical continuation to extend these functions to non-integral values of the number of servers, which has been widely used in the queueing theory related literature [59, 60].

$$\begin{cases} P_V = \frac{\rho^V (\Gamma(Q+1))^{-1} (Q^{V-Q})^{-1}}{\exp(\rho) \Gamma(Q, \rho) (\Gamma(Q))^{-1} + \rho^Q (1-a^{K-Q+1}) / (\Gamma(Q+1)(1-a))} \\ t_w = \frac{a \rho^Q [1-a^{V-Q+1} - (1-a)(V-Q+1)a^{V-Q}] K}{\gamma(1-a)^2 (1-P_V) \Gamma(Q+1) [\exp(\rho) \Gamma(Q, \rho) (\Gamma(Q))^{-1} + \rho^Q (1-a^{K-Q+1}) / (\Gamma(Q+1)(1-a))]} \end{cases} \quad (33)$$

where $\Gamma(\cdot)$ is the gamma function and $\Gamma(\cdot, \cdot)$ is the incomplete gamma function.

With the logit function (32), all model parameters involved in the bi-level charging infrastructure planning under plug-in charging and/or battery swapping are:

$$\Theta = \{\lambda_0, \alpha, \tau, \epsilon, \delta, c_0, l, s, p_e, A, B, C_{av}, C, Q, V, \phi_{vc}, \phi_{bs}\}, \quad (34)$$

⁸In the planning of battery swapping stations, the government only optimizes the number of battery swapping stations.

among which λ_0 , ϵ , c_0 , α , τ and A are parameters regarding the AMoD service; B is the scaling parameter of the vehicle searching time function; δ , l , s , C , Q and V are parameters that account for vehicles' driving and charging characteristics; p_e , C_{av} , ϕ_{vc} and ϕ_{bs} are cost factors that characterize the electricity cost, autonomous vehicle operating cost, and infrastructure costs of charging stations and battery swapping stations, respectively. Below we calibrate these parameters based on real-world data in New York City.

To calibrate the parameters regarding AMoD services, we take the TNC data for the Manhattan Central Business District (CBD) in New York City on a regular weekday. It records all ride-sourcing trips (e.g., origin, destination, pick-up time and drop-off time, etc.) that started from or ended in the Manhattan CBD area, from which we obtain that the average trip length is 2.4 miles and the average trip duration τ is 16.3 min. For the value of time α , the potential passenger demand λ_0 , and the parameters ϵ and c_0 in the logit model, we apply "reverse engineering" to infer their values so that the profit-maximizing solution given them matches the reported TNC data. For the scaling parameter A and B , we calibrate the passenger waiting time function (3) and vehicle searching time function (9) based on real-world geographic and traffic data of New York City using numerical simulation. The details of the calibration method can be found in Appendix D.

For vehicle charging, the involved model parameters are the average SoC δ , the electricity consuming rate l , the average charging speed s , the battery capacity C , the number of chargers/batteries within the battery swapping station Q , and the buffer size of the battery swapping station V . Autonomous electric TNC vehicles are assumed with an average electricity consumption of 0.25 kWh/mile when traveling on roads. Thus, the hourly electricity consuming rate l is

$$\frac{\text{average trip length}}{\text{average trip duration}} \times \text{average energy consumption} \times 60 = \frac{2.4}{16.3} * 0.25 * 60 = 2.21 \text{ kWh/hour.} \quad (35)$$

We further assume that the average SoC of vehicles that arrive at charging/battery swapping stations is $\delta = 10\%$. For the charging speed s and the battery capacity C , since charging technologies and battery technologies evolve over time, we set the nominal value as $s = 22 \text{ kW}$ (roughly 1.5 mile/min, Level 2 charging) and $C = 25 \text{ kWh}$ (a range of 100 miles). The impacts of different charging speeds and battery capacities will be investigated in Section 5.2 and Section 5.3, respectively. We further assume that for battery swapping stations, $Q = 6$ and $V = 20$.

For cost parameters p_e , C_{av} , ϕ_{vc} and ϕ_{bs} , we set $p_e = 0.12\$/\text{kWh}$ according to the reported average New York commercial electricity rate in February 2020 [61]. The investment and operating cost of autonomous vehicles consist of the cost of vehicle automation, coordination and maintenance, etc. We convert all capital costs of the autonomous vehicle to an hourly basis and denote C_{av} as the average hourly operating cost of an autonomous vehicle. We set $C_{av} = 15\$/\text{hour}$ as the nominal value such that the hourly operating cost of an autonomous vehicle is considerably lower than the average driver wage of human-driven TNC vehicles [49]. We transform the capital infrastructure costs into an hourly basis and denote ϕ_{vc} and ϕ_{bs} as the pro-rated investment cost plus the operating cost of charging stations and battery swapping stations, respectively. The infrastructure cost for charging stations is relatively low and is set to be $\phi_{vc} = 8\$/\text{hour}$, whereas the *per charger* cost of battery swapping stations ϕ_{bs} is usually several times higher than that of charging stations ϕ_{vc} , which is set as $\phi_{bs} = 40\$/\text{hour}$. In this case, the ratio of per charger cost of battery swapping stations compared to charging stations is $r = \frac{\phi_{bs}}{\phi_{vc}} = 5$.

Overall, the nominal values of model parameters for the numerical example of New York City are summarized below:

$$\begin{aligned} \lambda_0 &= 944/\text{min}, & \alpha &= 2.58, & \epsilon &= 0.155, & c_0 &= 15.48, & \tau &= 16.3 \text{ min}, & \delta &= 10\%, \\ s &= 22\text{kW}, & t_s &= 2 \text{ min}, & l &= 2.21\text{kW}, & p_e &= 0.12\$/\text{kWh}, & \beta_{1,2} &= 1, & A &= 230, & B &= 230, \\ C &= 25\text{kWh}, & Q &= 6, & V &= 15, & C_{av} &= 15\$/\text{h}, & \phi_{vc} &= 8\$/\text{hour}, & \phi_{bs} &= 40\$/\text{hour}, & r &= 5. \end{aligned}$$

5.2. Impacts of charging speed

This section investigates how charging speed affects the charging infrastructure planning and the market outcomes. Specifically, we vary the value of the model parameter s and solve the bi-level optimizations under distinct charging speeds for two different charging strategies, respectively.

Figure 3 presents the infrastructure planning of charging stations and battery swapping stations under different charging speeds. Numerical results show that for plug-in charging, as the charging speed improves, the number of charging stations increases (Figure 3a), the number of chargers per station reduces (Figure 3b), passenger surplus and TNC profit monotonically increases (Figure 3d-3f), and total social welfare also increases (Figure 3c). For battery swapping, as the charging speed improves, the government prefers to deploy fewer battery swapping stations (Figure 3a). In this case, the passenger surplus and social welfare monotonically increase (Figure 3c and Figure 3d), but the TNC profit initially increases and then drops (Figure 3e).

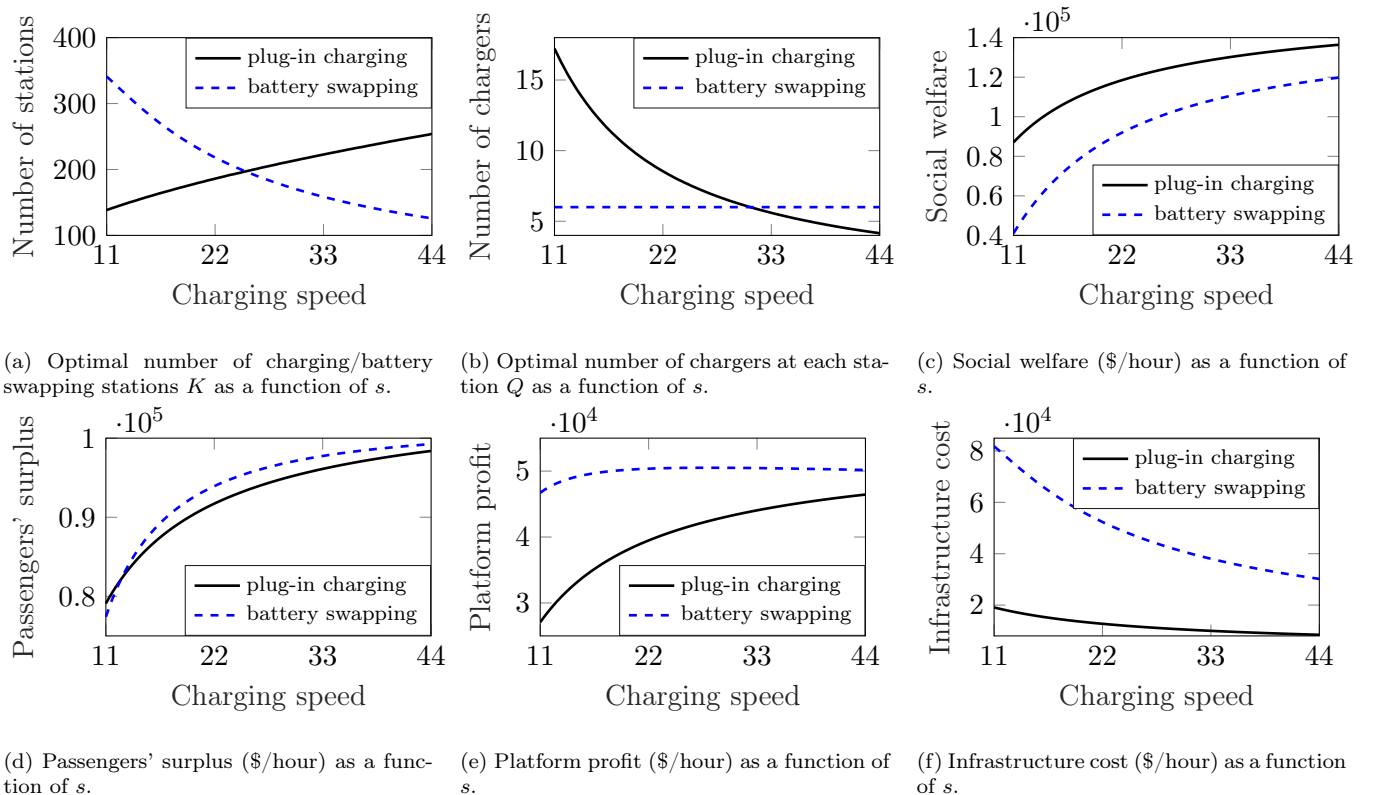
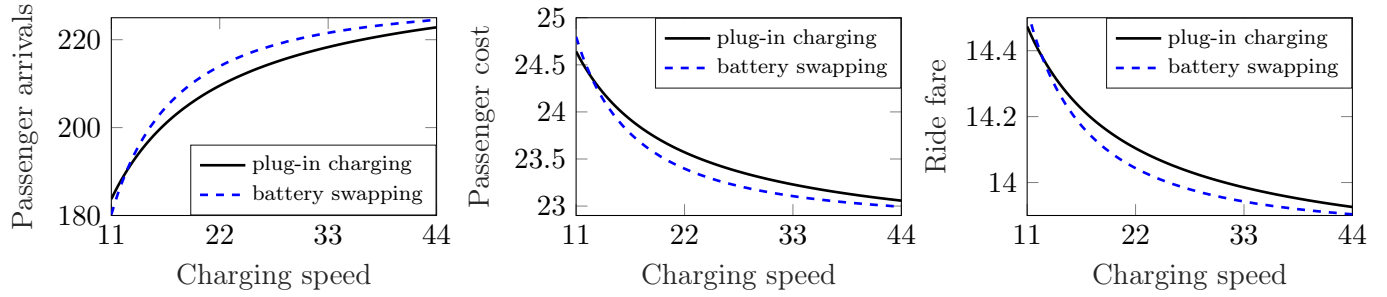
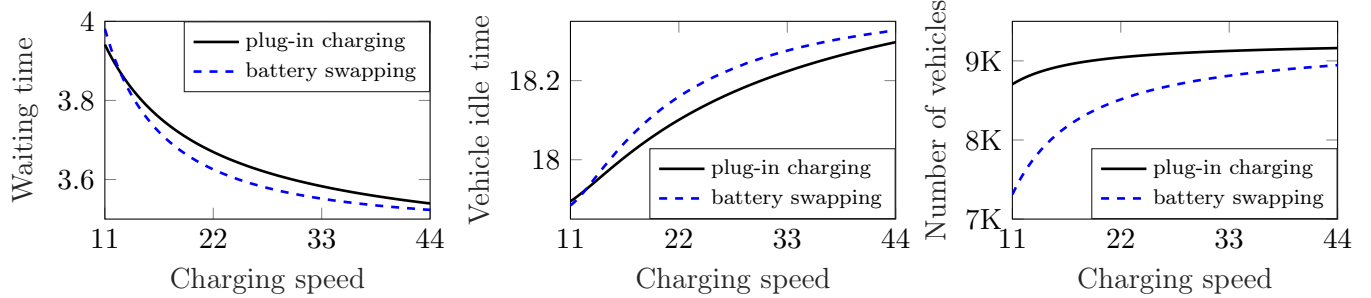


Figure 3: Charging infrastructure planning under different charging speeds. Black lines present the results when deploying charging stations; blue dashed lines show the results when deploying battery swapping stations.

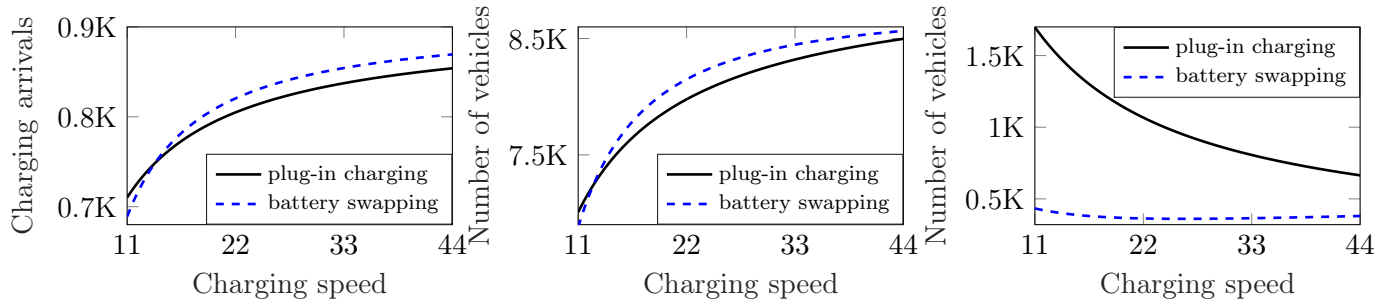
Figure 4 shows the market outcomes of the AMoD system under different charging speeds. As charging speed improves, the TNC lowers the ride fare (Figure 4c) and hires a larger fleet of vehicles (Figure 4f). This increases the vehicle idle time (Figure 4e) and the number of idle vehicles, resulting in a reduced passenger waiting time (Figure 4d). The total passenger travel cost drops with the charging speed (Figure 4b), and therefore more passengers choose the AMoD services (Figure 4a). This is the case for both plug-in charging and battery swapping. Figure 4g-4l illustrates the charging demand and the average time spent on charging for vehicles under the two charging strategies. Numerical results show that the charging demand (Figure 4g) and the number of operating vehicles (Figure 4h) under two distinct charging strategies monotonically increase with the charging speed. For plug-in charging, as charging speed improves, the vehicle searching time reduces (Figure 4j), the vehicle waiting time slightly decreases (Figure 4k), and the average vehicle charging time sharply drops (Figure 4l). Under battery swapping, there is a small number of non-operating



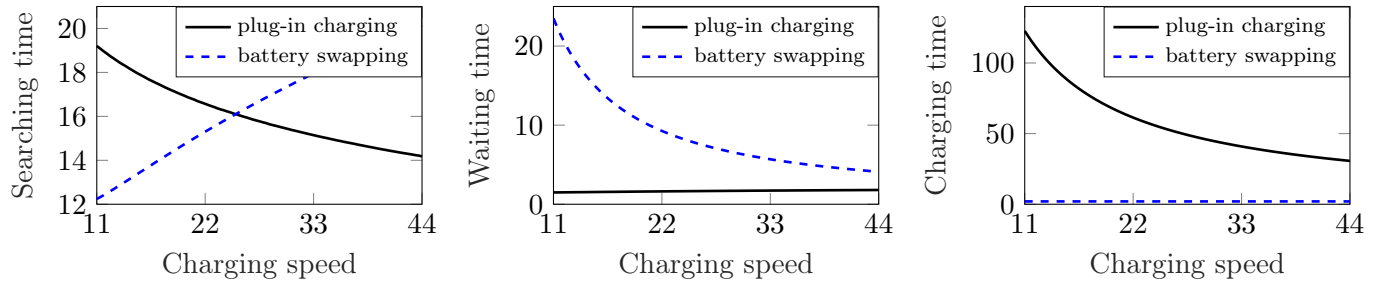
(a) Passenger arrival rate λ (per minute) as a function of s . (b) Passenger travel cost c (\$/trip) as a function of s . (c) Per-trip ride fare p_f (\$/trip) as a function of s .



(d) Passenger waiting time w^c (minute) as a function of s . (e) Vehicle idle time w^v (minute) as a function of s . (f) Total number of vehicles N as a function of s .



(g) Charging arrival rate γ (per hour) as a function of s . (h) Number of operating vehicles N_1 as a function of s . (i) Number of non-operating vehicles N_2 as a function of s .



(j) Vehicle searching time t_m (minute) as a function of s . (k) Vehicle waiting time t_w (minute) as a function of s . (l) Vehicle charging time t_s (minute) as a function of s .

Figure 4: Market outcomes on electrified AMoD services under different charging speed. Black lines present the results when charging vehicles; blue dashed lines show the results when swapping batteries.

vehicles, which experience a little change with charging speed (Figure 4i). As the charging speed improves, the vehicle searching time rises with the charging speed (Figure 4j), the vehicle waiting time reduces as the charging speed increases (Figure 4k), and the vehicle charging time (i.e., the service time of battery

swapping) remains constant under different charging speeds (Figure 4l).

Overall, we summarize the key findings as follows:

- When deploying charging stations for AMoD services, improved charging speed results in a transformation of the infrastructure deployment from *sparingly distributed large stations* to *densely distributed small stations* (Figure 3a and Figure 3b).
- When deploying battery swapping stations for AMoD services, improved charging speed reduces the need for charging infrastructure (Figure 3a) and leads to a smaller number of battery swapping stations.
- Under the strategy of plug-in charging, improved charging speed brings a Pareto improvement: a higher charging speed always leads to a higher passenger surplus (Figure 3d), a higher platform profit (Figure 3e) and increased social welfare (Figure 3c).
- Under the strategy of battery swapping, passengers always benefit from the improved charging technology (Figure 3d) and the social welfare monotonically increases with the charging speed (Figure 3c). However, the TNC may get hurt when the charging speed is relatively high (Figure 3e).

To explain the impacts of charging speed on charging infrastructure planning decisions, we first note that improving charging speed directly increases the service rate of each charger. This motivates the government to reduce the total supply of chargers (i.e., KQ) for cost-saving (Figure 3f). Specifically, for battery swapping stations, the government has to reduce the number of battery swapping stations K as Q is fixed (Figure 3a). On the other hand, for plug-in charging, the government is flexible in determining the number of charging stations K and the number of chargers per station Q . In this case, it faces a trade-off: on the one hand, it can build a large number of small charging stations (i.e., large K and small Q), which leads to densely distributed charging infrastructures. This reduces the time vehicles search for/travel to nearby charging stations. On the other hand, it can build a small number of large charging stations (i.e., small K and large Q), which leads to sparsely distributed large charging centers. This increases the service capability of each charging station and results in a shorter waiting time at stations. The government should carefully control the knobs to achieve a balance between the vehicle searching time to stations and the vehicle waiting time at stations. As the charging speed improves, it helps to curb the vehicle waiting time at stations. In this case, the improved charging speed alters the trade-off incurred by infrastructure deployment: the marginal effect of allocating more chargers per station on reducing vehicle waiting time diminishes, and the vehicle searching time gradually becomes the bottleneck. Consequently, the government builds more stations and reduces the number of chargers at each station, which leads to the transformation of the infrastructure deployment from *sparingly distributed large stations* to *densely distributed small stations*.

A counter-intuitive result is that increased charging speed may not always lead to a higher TNC profit: in certain regimes, the TNC profit reduces as charging speed improves. This suggests that, unlike plug-in charging, where all stakeholders benefit from the increased charging speed, the TNC platform may not necessarily welcome fast charging technology when battery swapping stations are deployed. We comment that such a difference is due to the limited flexibility of battery swapping stations for AMoD services. In the deployment of charging stations, the government is flexible to jointly control the number of charging stations K and the number of chargers per station Q . The improved charging speed promotes the government to lower the total supply of charging infrastructures for cost-saving. In this case, although the total supply of charging infrastructures reduces, the government builds fewer charging stations and allocates more chargers to each station to balance the vehicle searching time and the vehicle waiting time, both the vehicle searching time (Figure 4j), the vehicle waiting time (Figure 4k), and the vehicle charging time (Figure 4l) reduce as charging speed increases. This leads to a more efficient use of the TNC fleet, which benefits the TNC platform. On the other hand, for battery swapping, the government can only control the total number of

stations K to adjust the supply of charging infrastructures⁹. As charging speed increases, the government has to decrease the number of battery swapping stations to reduce infrastructure costs, which leads to a sparser distribution of battery swapping stations and increases the vehicle searching time to stations. Although improving charging speed increases each battery charger’s service rate and helps curb the vehicle waiting time at battery swapping stations, the reduced supply of charging infrastructures also leads to a longer vehicle searching time to stations. When the negative effect of reduced charging infrastructure supply dominates, the vehicle searching time significantly increases (Figure 4j), the number of non-operating vehicles increases (Figure 4i), and the fleet utilization rate drops. To maintain the operation of AMoD services, the TNC needs to recruit a larger fleet of vehicles, which leads to increased vehicle operating costs and reduced profit.

5.3. Impacts of battery capacity

This section investigates the impacts of battery capacity on the charging infrastructure planning and AMoD market. To this end, we will solve the bi-level optimization under distinct values of the model parameter C under different charging strategies and compare the corresponding results.

Figure 5 presents the infrastructure planning of charging stations and battery swapping stations under different battery capacities. Numerical results show that for both charging strategies, increased battery capacity will lead to a larger passenger surplus (Figure 5d), larger platform profit (Figure 5e), smaller infrastructure cost (Figure 5f), and large social welfare (Figure 5c). However, for plug-in charging, increased battery capacity leads to a smaller number of charging stations (Figure 5a) but a larger number of chargers at each station (Figure 5b), whereas for battery swapping, increased battery capacity leads to a reduced number of battery swapping stations (Figure 5a).

Figure 6 presents the impacts of battery capacity on the AMoD system. Under both plug-in charging and battery swapping, as the battery capacity increases, the TNC reduces the ride fare (Figure 6c) and recruits more autonomous vehicles (Figure 6f). The vehicle idle time increases (Figure 6e), which lowers the passenger waiting time and improves the service quality (Figure 6d). Therefore, the total passenger cost reduces with battery capacity (Figure 6b), attracting more passengers to choose AMoD services (Figure 6a).

Figure 7 shows the charging demand and the average time spent on charging for TNC vehicles under the two charging strategies. Numerical results show that under both strategies of vehicle charging and battery swapping, as the battery capacity increases, the charging demand largely drops (Figure 7a), and the number of operating vehicles increases (Figure 7b). The number of non-operating vehicles under battery swapping significantly decreases, while that under plug-in charging has a relatively small reduction (Figure 7c). More specifically, under plug-in charging, the number of searching vehicles reduces (Figure 7d), the number of waiting vehicles decreases (Figure 7e), and the number of charging vehicles remains almost steady (Figure 7f). As for distinct time periods in the vehicle’s charging process, we find that the vehicle searching time to stations increases with the battery capacity (Figure 7g). Vehicles also have a longer waiting time at charging stations (Figure 7h), and the vehicle charging time linearly increases with the battery capacity (Figure 7i). On the other hand, under battery swapping, the number of searching vehicles declines (Figure 7d), whereas the number of waiting vehicles at stations slightly increases (Figure 7e). The number of charging vehicles keeps decreasing with battery capacity and becomes close to zero (Figure 7f). Correspondingly, the vehicle searching time has a slight increase (Figure 7g), the vehicle waiting time at battery swapping stations rises

⁹As mentioned in Section 4.2, the battery swapping station typically has a fixed number of chargers Q , which is difficult to adjust in short term because of its closed structure, and because of the need of standardization for the convenience of mass production.

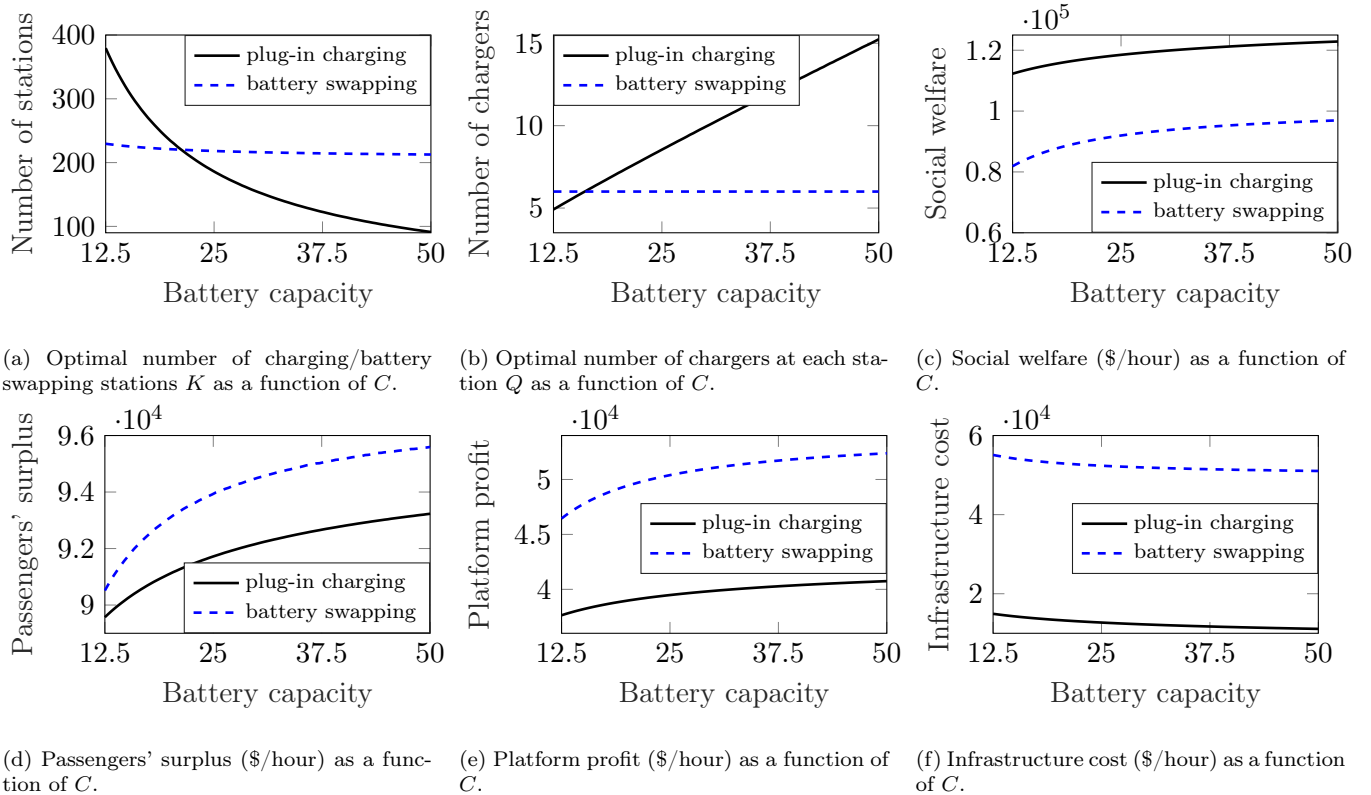


Figure 5: Charging infrastructure planning under different battery capacities. Black lines present the results when deploying charging stations; blue dashed lines show the results when deploying battery swapping stations.

significantly (Figure 7h), and the vehicle charging time (i.e., the service time of battery swapping) still remains constant (Figure 7i).

The key findings regarding the impacts of battery capacity are outlined below:

- When deploying charging stations for AMoD systems, the increased battery capacity results in a transformation of infrastructure deployment from *densely distributed small stations* to *sparsely distributed large stations* (Figure 5a and Figure 5b).
- When deploying battery swapping stations for AMoD systems, the enlarged battery capacity lowers the supply of charging infrastructure (Figure 5a and Figure 5b).
- Under both strategies of vehicle charging and battery swapping, improved battery capacity leads to a Pareto improvement: passengers enjoy higher surplus (Figure 5d), the TNC earns increased profit (Figure 5e), and the government produces higher social welfare (Figure 5c).

Analogous to the impacts of charging speed, the improved battery capacity reduces the need for charging infrastructures under both charging strategies. This is intuitive because increasing battery capacity extends vehicles' operating hours and directly reduces the demand for recharging electricity. The marginal benefit of offering charging infrastructures diminishes as the charging demand drops. Therefore, the government cuts down the total supply of charging infrastructures to save infrastructure costs. When planning battery swapping stations, due to its standard configuration, the government would offer fewer battery swapping stations for cost-saving as battery capacity enlarges (Figure 5a). On the other hand, when deploying charging stations, although the total number of chargers declines (Figure 5f), the improved battery capacity transforms the infrastructure deployment from *densely distributed small stations* to *sparsely distributed*

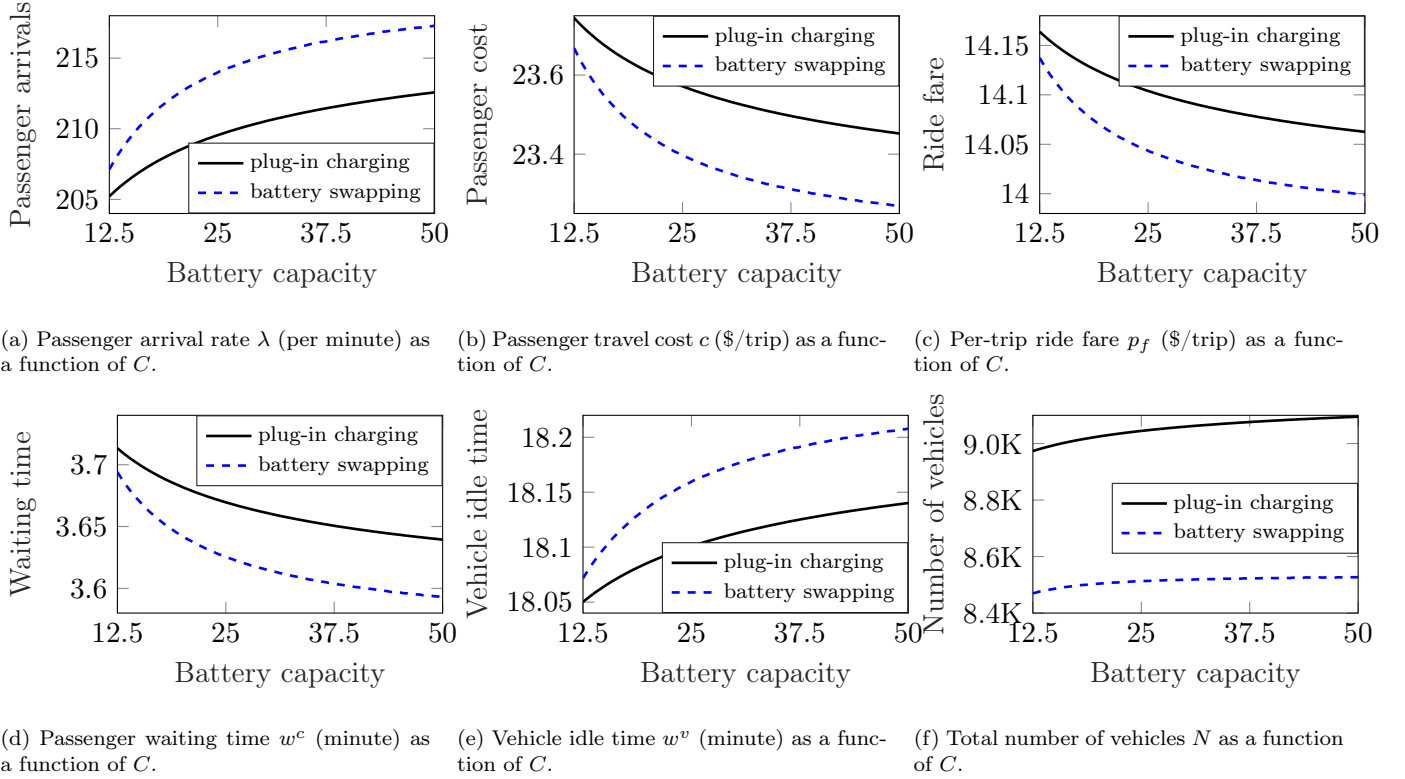


Figure 6: Market outcomes on electrified AMoD services under different battery capacities. Black lines present the results when charging vehicles; blue dashed lines show the results when swapping batteries.

large stations (Figure 5a and Figure 5b), which is contrary to the transformation caused by improved charging speed (Figure 3a and Figure 3b). Similarly, this can be explained as a consequence of the trade-off between the vehicle searching time and the vehicle waiting time. As battery capacity increases, the charging demand largely drops (Figure 7a), which lowers the arrival rate of vehicles at charging stations and alleviates the congestion at stations. However, a larger battery capacity also requires a longer time to charge the depleted battery (Figure 7i). This raises the service/occupied time of each electric vehicle charger and extends vehicles' waiting time for vacant chargers. In this case, expanding battery capacity breaks the balance achieved by infrastructure deployment: the vehicle waiting time at stations increases with battery capacity and becomes the bottleneck. To achieve the optimal trade-off, the government reduces the number of charging stations and deploys more chargers at each station, which leads to the transformation of infrastructure deployment from *densely distributed small stations* to *sparingly distributed large stations*. Under such transformation, although the vehicle searching time increases owing to the reduced density of charging stations (Figure 7g), the vehicle waiting time remains at a relatively low level (Figure 7h). Overall, given the reduced charging demand, both the number of searching vehicles (Figure 7d) and waiting vehicles (Figure 7e) decrease as battery capacity. This improves the fleet utilization rate and brings higher profit for the TNC.

5.4. Comparison of plug-in charging and battery swapping

This section compares two distinct charging strategies under different infrastructure costs, charging speeds, and battery capacities. In particular, we fix the per charger cost ratio of battery swapping stations and charging stations as $r = \frac{\phi_{bs}}{\phi_{vc}} = 5$, and decrease the per charger operating cost of battery swapping stations ϕ_{bs} from 40\$/hour to 20\$/hour to reflect the trend of reduced infrastructure costs over time. The bi-level optimization for vehicle charging and battery swapping will be solved and compared under distinct

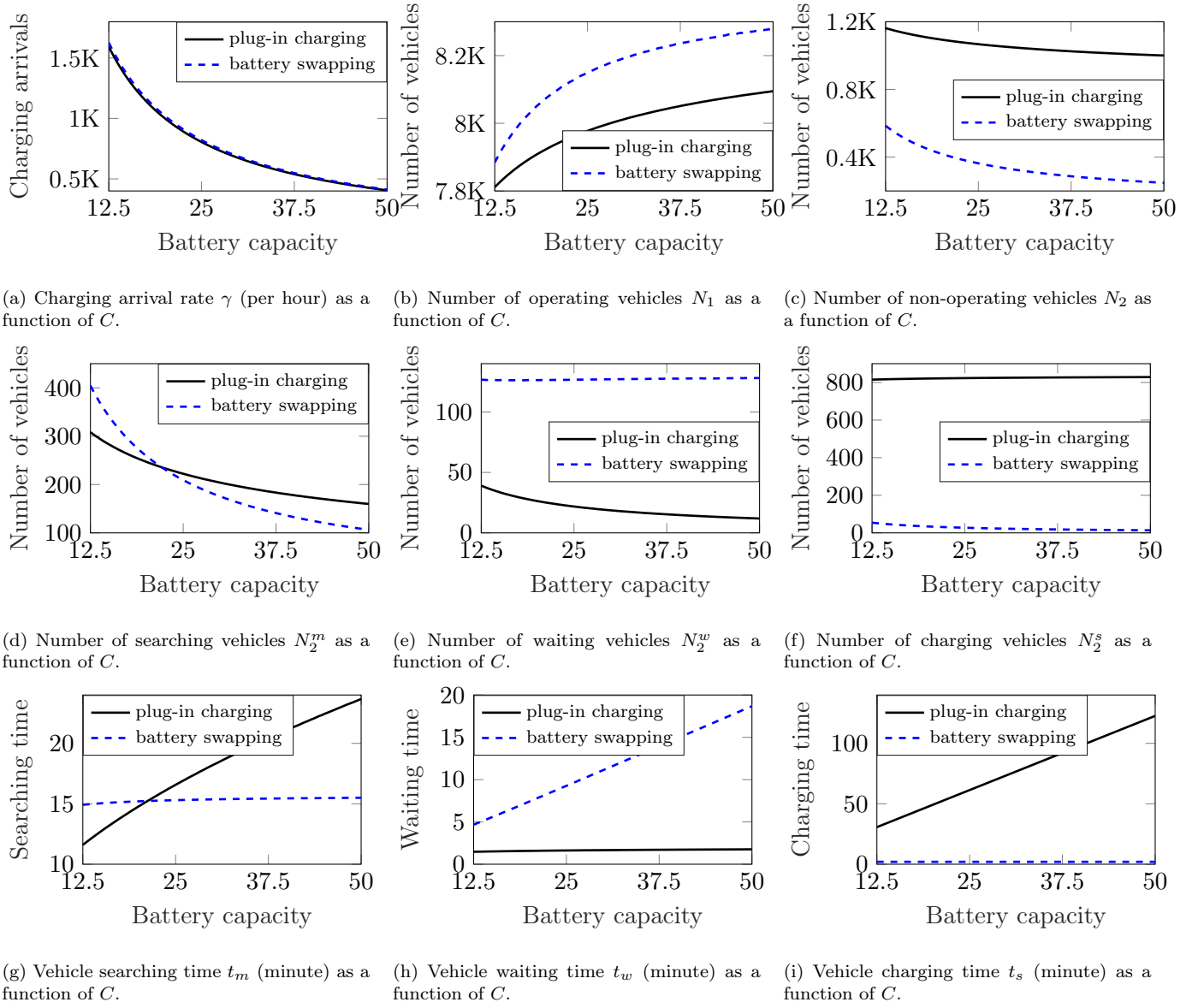


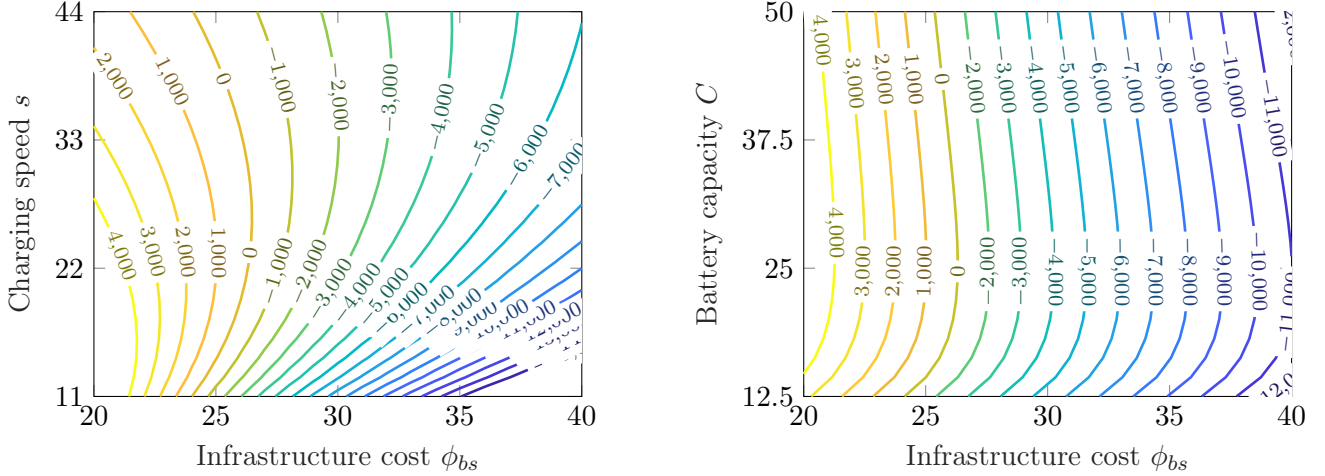
Figure 7: Market outcomes on vehicle charging under different battery capacities. Black lines present the results when charging vehicles; blue dashed lines show the results when swapping batteries.

combinations of model parameters ϕ_{bs} , s , and C .

Figure 8 presents the difference in social welfare between battery swapping and plug-in charging under distinct technology conditions. Specifically, Figure 8a shows the contour plot of social welfare difference between battery swapping and plug-in charging under distinct combinations of infrastructure costs and charging speeds. Figure 8b illustrates the contour plot of social welfare differences under distinct infrastructure costs and battery capacities. Overall, several key findings are summarized below:

- As the infrastructure cost reduces, the advantage of battery swapping over plug-in charging strengthens. There exists a break-even cost ratio below which battery swapping is superior to plug-in charging in promoting societal benefits.
- Under a fixed infrastructure cost, when the charging speed is either very small or very large, and advantage of battery swapping diminishes. Similarly, the advantage of battery swapping initially

increases and then diminishes as battery capacity increases.



(a) The social welfare difference between battery swapping and vehicle charging under distinct r and s .

(b) The social welfare difference between battery swapping and vehicle charging under distinct r and C .

Figure 8: The social welfare difference between battery swapping and vehicle charging under different cost ratios, charging speeds, and battery capacities.

As the technology evolves and infrastructure develops, the marginal cost of supplying charging infrastructures reduces, which enables the government to deploy more charging stations and battery swapping stations for electrified AMoD services. The increased charging infrastructure supply improves the charging capability and reduces the vehicle searching time and vehicle waiting time for charging. However, the overlong charging time is still the major bottleneck in plug-in charging, which restricts the benefits of improving the charging supply. As the infrastructure costs reduce, the advantage of battery swapping over plug-in charging gradually emerges and becomes more and more significant. For example, in the numerical example with the charging speed of 22kW (Level 2 charging), the battery capacity of 25kWh (100 miles vehicle range), and the fixed cost ratio of 5, when the infrastructure cost of battery swapping ϕ_{bs} is below 25\$/hour (the corresponding infrastructure cost for plug-in charging $\phi_{vc} = 5$ \$/hour), battery swapping for electric AMoD services produces higher social welfare than plug-in charging. This provides technical guidance for the government on how to plan charging infrastructures according to distinct technological configurations.

An interesting result is that the advantage of battery swapping initially strengthens as the charging speed/battery capacity improves but eventually diminishes as the charging speed/battery capacity further increases. We argue that this is again due to the difference in the flexibility of infrastructure deployment when planning charging stations and battery swapping stations. When the charging speed/battery capacity is relatively low, the government must supply a large amount of charging infrastructure (either charging stations or battery swapping stations) to accommodate the AMoD services. Given the high supply of charging infrastructure, the costs of charging infrastructure dominate social welfare, and the government expends much more infrastructure costs when deploying battery swapping stations than deploying charging stations (see Figure 3f and Figure 5f). As charging speed/battery capacity increases, the marginal benefit of supplying charging infrastructures reduces, and therefore the government lowers the charging infrastructure supply. The difference in infrastructure costs between the two charging strategies decreases, and the advantages of battery swapping over plug-in charging become increasingly significant. However, as mentioned before, the reduced charging infrastructure supply also negatively impacts and suppresses the TNC profit. When deploying charging stations, the government has the flexibility to determine the size of charging stations, by which the negative impacts of reduced charging infrastructure supply can be largely mitigated. On the other hand, when deploying battery swapping stations, the limited flexibility

of infrastructure deployment magnifies the negative effects of reduced infrastructure supply. As charging speed/battery capacity increases, such negative effects gradually become the dominant factor and make battery swapping less advantageous compared to vehicle charging.

6. Conclusion

This paper investigates two prevalent charging solutions, plug-in charging and battery swapping, and the corresponding charging infrastructure planning for charging electric AMoD systems. An economic equilibrium model is developed to understand and reveal the operational mechanism of the TNC's electric AMoD system. The incentives of passengers, the operating/charging shift of TNC vehicles, and the balance of energy are captured, and vehicle charging processes at charging stations and battery swapping stations are characterized by queueing theory. A bi-level optimization framework is established to capture the intimate correlations between the government's charging infrastructure planning and the TNC's operation of the electric AMoD system. The upper-level social welfare maximization for the government and the lower-level profit maximization for the TNC are formulated, in which the structural difference of charging infrastructures and the flexibility of infrastructure deployment are considered. The government's optimal infrastructure deployment, the corresponding TNC's profit-maximizing operational strategies, and the market outcomes are obtained by solving the bi-level optimization problem.

We use the established bi-level optimization framework to investigate the impacts of involved charging technologies on the government's charging infrastructure planning and the TNC's operation of electric AMoD systems. We find that the evolution of charging technologies will reduce the need for charging infrastructures under both plug-in charging and battery swapping. In the planning of charging stations, the improved charging speed leads to a transformation of infrastructure deployment from *sparsely distributed large stations* to *densely distributed small stations*, while the enlarged battery capacity transforms the infrastructure deployment from *densely distributed small stations* to *sparsely distributed large stations*. The underlying reason is that the evolving charging technologies alter the trade-off between vehicle searching time and vehicle waiting time and promote the government to adjust the infrastructure deployment. We also show that the evolution of charging technologies has distinct impacts on the TNC's operation of electric AMoD systems under distinct charging solutions. The improved charging speed always leads to increased TNC profit under plug-in charging, while the TNC may get hurt when the charging speed is relatively high under battery swapping. This demonstrates that the limited flexibility of infrastructure deployment of battery swapping stations restricts the potential of battery swapping for electric AMoD systems. We further compare plug-in charging and battery swapping for charging electric AMoD systems under distinct infrastructure costs. We find that there exists a break-even cost ratio at which battery swapping is equivalent to plug-in charging in promoting social welfare.

This paper delivers a comprehensive economic analysis of the operation of the electric AMoD system and the corresponding charging infrastructure planning. Under the proposed bi-level optimization framework, we evaluate and compare two prevalent charging solutions plug-in charging and battery swapping separately, and investigate the impacts of evolving charging technologies on the charging infrastructure planning and the market outcomes at the aggregate level. One future extension is considering the synergy between plug-in charging and battery swapping for charging electric AMoD systems. Another future direction would be extending the current economic equilibrium model to a network equilibrium model and optimizing the zonal level charging infrastructure deployment to account for the spatial heterogeneity of AMoD services. We hope this work could stimulate more discussion in electrified, automated, and shared mobility for efficient and sustainable future transportation.

Acknowledgments

This research was supported by the Hong Kong Research Grants Council under project 26200420, project 16202922, and the National Science Foundation of China under project 72201225.

References

- [1] Waymo. Waymo one. <https://waymo.com/intl/zh-cn/waymo-one/>, 2022.
- [2] Brittany Chang. Chinese uber competitor didi unveiled a futuristic ev made specifically for ride-sharing — see the d1. <https://www.businessinsider.com/didi-unveiled-the-d1-electric-vehicle-made-for-ridesharing-2020-12>, 2018.
- [3] T Donna Chen, Kara M Kockelman, and Josiah P Hanna. Operations of a shared, autonomous, electric vehicle fleet: Implications of vehicle & charging infrastructure decisions. *Transportation Research Part A: Policy and Practice*, 94:243–254, 2016.
- [4] Gordon S Bauer, Jeffery B Greenblatt, and Brian F Gerke. Cost, energy, and environmental impact of automated electric taxi fleets in manhattan. *Environmental science & technology*, 52(8):4920–4928, 2018.
- [5] Erick C Jones and Benjamin D Leibowicz. Contributions of shared autonomous vehicles to climate change mitigation. *Transportation Research Part D: Transport and Environment*, 72:279–298, 2019.
- [6] Tesla. Supercharger. <https://www.tesla.com/supercharger>, 2022.
- [7] Mark Kane. China: Nio celebrates 900th battery swap station. <https://insideevs.com/news/581626/china-nio-900-battery-swap-stations/>, 2022.
- [8] International Electrotechnical Commission. Iec 61851-1:2017: Electric vehicle conductive charging system - part 1: General requirements. <https://webstore.iec.ch/publication/33644>, 2021.
- [9] Hao Liang, Isha Sharma, Weihua Zhuang, and Kankar Bhattacharya. Plug-in electric vehicle charging demand estimation based on queueing network analysis. In *2014 IEEE PES General Meeting/Conference & Exposition*, pages 1–5. IEEE, 2014.
- [10] Ke Zhang, Yuming Mao, Supeng Leng, Yan Zhang, Stein Gjessing, and Danny HK Tsang. Platoon-based electric vehicles charging with renewable energy supply: A queueing analytical model. In *2016 IEEE International Conference on Communications (ICC)*, pages 1–6. IEEE, 2016.
- [11] Yongmin Zhang, Pengcheng You, and Lin Cai. Optimal charging scheduling by pricing for ev charging station with dual charging modes. *IEEE Transactions on Intelligent Transportation Systems*, 20(9):3386–3396, 2018.
- [12] Bingqing Liu, Theodoros P Pantelidis, Stephanie Tam, and Joseph YJ Chow. An electric vehicle charging station access equilibrium model with m/d/c queueing. *International Journal of Sustainable Transportation*, pages 1–17, 2022.
- [13] Angelos Aveklouris, Yorie Nakahira, Maria Vlasidou, and Bert Zwart. Electric vehicle charging: a queueing approach. *ACM SIGMETRICS Performance Evaluation Review*, 45(2):33–35, 2017.
- [14] Sajad Esmailirad, Ali Ghiasian, and Abdorreza Rabiee. An extended m/m/k/k queueing model to analyze the profit of a multiservice electric vehicle charging station. *IEEE Transactions on Vehicular Technology*, 70(4):3007–3016, 2021.

- [15] Xiaoqi Tan, Bo Sun, and Danny HK Tsang. Queueing network models for electric vehicle charging station with battery swapping. In *2014 IEEE International Conference on Smart Grid Communications (SmartGridComm)*, pages 1–6. IEEE, 2014.
- [16] Bo Sun, Xiaoqi Tan, and Danny HK Tsang. Optimal charging operation of battery swapping and charging stations with qos guarantee. *IEEE Transactions on Smart Grid*, 9(5):4689–4701, 2017.
- [17] Xiaoqi Tan, Bo Sun, Yuan Wu, and Danny HK Tsang. Asymptotic performance evaluation of battery swapping and charging station for electric vehicles. *Performance Evaluation*, 119:43–57, 2018.
- [18] Farhad Imani, Tongdan Jin, and Lihui Bai. Modeling and simulation of hybrid battery swapping stations with fast onboard charging. In *2016 Industrial and Systems Engineering Research Conference*, pages 1–8, 2016.
- [19] Fiona Sloothaak, James Cruise, Seva Shneer, Maria Vlasidou, and Bert Zwart. Complete resource pooling of a load-balancing policy for a network of battery swapping stations. *Queueing Systems*, 99(1):65–120, 2021.
- [20] Rick Zhang, Federico Rossi, and Marco Pavone. Model predictive control of autonomous mobility-on-demand systems. In *2016 IEEE International Conference on Robotics and Automation (ICRA)*, pages 1382–1389. IEEE, 2016.
- [21] Nathaniel Tucker, Berkay Turan, and Mahnoosh Alizadeh. Online charge scheduling for electric vehicles in autonomous mobility on demand fleets. In *2019 IEEE Intelligent Transportation Systems Conference (ITSC)*, pages 226–231. IEEE, 2019.
- [22] Riccardo Iacobucci, Benjamin McLellan, and Tetsuo Tezuka. Optimization of shared autonomous electric vehicles operations with charge scheduling and vehicle-to-grid. *Transportation Research Part C: Emerging Technologies*, 100:34–52, 2019.
- [23] Felix Boewing, Maximilian Schiffer, Mauro Salazar, and Marco Pavone. A vehicle coordination and charge scheduling algorithm for electric autonomous mobility-on-demand systems. In *2020 American Control Conference (ACC)*, pages 248–255. IEEE, 2020.
- [24] Berkay Turan, Ramtin Pedarsani, and Mahnoosh Alizadeh. Dynamic pricing and fleet management for electric autonomous mobility on demand systems. *Transportation Research Part C: Emerging Technologies*, 121:102829, 2020.
- [25] Zhaohao Ding, Wenrui Tan, Wei-Jen Lee, Xuyang Pan, and Shiqiao Gao. Integrated operation model for autonomous mobility-on-demand fleet and battery swapping station. *IEEE Transactions on Industry Applications*, 57(6):5593–5602, 2021.
- [26] Zhaohao Ding, Wenrui Tan, Wenbing Lu, and Wei-Jen Lee. Quality-of-service aware battery swapping navigation and pricing for autonomous mobility on demand system. *IEEE Transactions on Industrial Informatics*, 2022.
- [27] Liang Ni, Bo Sun, Su Wang, and Danny HK Tsang. Dynamic pricing mechanism design for electric mobility-on-demand systems. *IEEE Transactions on Intelligent Transportation Systems*, 2021.
- [28] Berkay Turan, Nathaniel Tucker, and Mahnoosh Alizadeh. Smart charging benefits in autonomous mobility on demand systems. In *2019 IEEE Intelligent Transportation Systems Conference (ITSC)*, pages 461–466. IEEE, 2019.
- [29] Federico Rossi, Ramon Iglesias, Mahnoosh Alizadeh, and Marco Pavone. On the interaction between autonomous mobility-on-demand systems and the power network: Models and coordination algorithms. *IEEE Transactions on Control of Network Systems*, 7(1):384–397, 2019.

- [30] Berkay Turan and Mahnoosh Alizadeh. Competition in electric autonomous mobility on demand systems. *IEEE Transactions on Control of Network Systems*, 2021.
- [31] Heeseung Bang and Andreas A Malikopoulos. Congestion-aware routing, rebalancing, and charging scheduling for autonomous electric mobility-on-demand system. *arXiv preprint arXiv:2110.04911*, 2021.
- [32] Fang He, Di Wu, Yafeng Yin, and Yongpei Guan. Optimal deployment of public charging stations for plug-in hybrid electric vehicles. *Transportation Research Part B: Methodological*, 47:87–101, 2013.
- [33] Fang He, Yafeng Yin, and Jing Zhou. Deploying public charging stations for electric vehicles on urban road networks. *Transportation Research Part C: Emerging Technologies*, 60:227–240, 2015.
- [34] Zhihong Zhu, Ziyou Gao, Jianfeng Zheng, and Haoming Du. Charging station planning for plug-in electric vehicles. *Journal of Systems Science and Systems Engineering*, 27(1):24–45, 2018.
- [35] Mohammadreza Kavianiipour, Fatemeh Fakhroosavi, Harprinderjot Singh, Mehrnaz Ghamami, Ali Zockaie, Yanfeng Ouyang, and Robert Jackson. Electric vehicle fast charging infrastructure planning in urban networks considering daily travel and charging behavior. *Transportation Research Part D: Transport and Environment*, 93:102769, 2021.
- [36] Gordon S Bauer, Amol Phadke, Jeffery B Greenblatt, and Deepak Rajagopal. Electrifying urban ridesourcing fleets at no added cost through efficient use of charging infrastructure. *Transportation Research Part C: Emerging Technologies*, 105:385–404, 2019.
- [37] Tai-Yu Ma and Yumeng Fang. Optimal queueing-based vehicle charging scheduling and assignment for dynamic electric ridepooling service. In *International Conference on Operations Research (OR2021)*, 2021.
- [38] Ho-Yin Mak, Ying Rong, and Zuo-Jun Max Shen. Infrastructure planning for electric vehicles with battery swapping. *Management science*, 59(7):1557–1575, 2013.
- [39] Jun Yang, Fang Guo, and Min Zhang. Optimal planning of swapping/charging station network with customer satisfaction. *Transportation Research Part E: Logistics and Transportation Review*, 103:174–197, 2017.
- [40] U Sultana, Azhar B Khairuddin, Beenish Sultana, Nadia Rasheed, Sajid Hussain Qazi, and Nimra Riaz Malik. Placement and sizing of multiple distributed generation and battery swapping stations using grasshopper optimizer algorithm. *Energy*, 165:408–421, 2018.
- [41] Bo Sun, Xu Sun, Danny HK Tsang, and Ward Whitt. Optimal battery purchasing and charging strategy at electric vehicle battery swap stations. *European Journal of Operational Research*, 279(2):524–539, 2019.
- [42] Yanni Liang, Hua Cai, and Guilin Zou. Configuration and system operation for battery swapping stations in beijing. *Energy*, 214:118883, 2021.
- [43] Benjamin Loeb, Kara M Kockelman, and Jun Liu. Shared autonomous electric vehicle (saev) operations across the austin, texas network with charging infrastructure decisions. *Transportation Research Part C: Emerging Technologies*, 89:222–233, 2018.
- [44] Reza Vosooghi, Jakob Puchinger, Joschka Bischoff, Marija Jankovic, and Anthony Vouillon. Shared autonomous electric vehicle service performance: Assessing the impact of charging infrastructure. *Transportation Research Part D: Transport and Environment*, 81:102283, 2020.

- [45] Mustafa Lokhandwala and Hua Cai. Siting charging stations for electric vehicle adoption in shared autonomous fleets. *Transportation Research Part D: Transport and Environment*, 80:102231, 2020.
- [46] Justin Luke, Mauro Salazar, Ram Rajagopal, and Marco Pavone. Joint optimization of autonomous electric vehicle fleet operations and charging station siting. In *2021 IEEE International Intelligent Transportation Systems Conference (ITSC)*, pages 3340–3347. IEEE, 2021.
- [47] George W Douglas. Price regulation and optimal service standards: The taxicab industry. *Journal of Transport Economics and Policy*, pages 116–127, 1972.
- [48] Richard Arnott. Taxi travel should be subsidized. *Journal of Urban Economics*, 40(3):316–333, 1996.
- [49] Sen Li, Hamidreza Tavafoghi, Kameshwar Poola, and Pravin Varaiya. Regulating tncs: Should uber and lyft set their own rules? *Transportation Research Part B: Methodological*, 129:193–225, 2019.
- [50] Liteng Zha, Yafeng Yin, and Zhengtian Xu. Geometric matching and spatial pricing in ride-sourcing markets. *Transportation Research Part C: Emerging Technologies*, 92:58–75, 2018.
- [51] Yongjun Ahn and Hwasoo Yeo. An analytical planning model to estimate the optimal density of charging stations for electric vehicles. *PloS one*, 10(11):e0141307, 2015.
- [52] Jinwoo Lee and Samer Madanat. Optimal design of electric vehicle public charging system in an urban network for greenhouse gas emission and cost minimization. *Transportation Research Part C: Emerging Technologies*, 85:494–508, 2017.
- [53] Zhijie Lai and Sen Li. On-demand valet charging for electric vehicles: Economic equilibrium, infrastructure planning and regulatory incentives. *Transportation Research Part C: Emerging Technologies*, 140:103669, 2022.
- [54] Arnold O Allen. *Probability, statistics, and queueing theory*. Gulf Professional Publishing, 1990.
- [55] Raif O Onvural. Survey of closed queueing networks with blocking. *ACM Computing Surveys (CSUR)*, 22(2):83–121, 1990.
- [56] Ying Zhang, Yanhao Wang, Fanyu Li, Bin Wu, Yao-Yi Chiang, and Xin Zhang. Efficient deployment of electric vehicle charging infrastructure: Simultaneous optimization of charging station placement and charging pile assignment. *IEEE Transactions on Intelligent Transportation Systems*, 22(10):6654–6659, 2020.
- [57] Zhonghao Zhao, Carman KM Lee, and Jiage Huo. Ev charging station deployment on coupled transportation and power distribution networks via reinforcement learning. *Energy*, 267:126555, 2023.
- [58] Jing Gao, Sen Li, and Hai Yang. Shared parking for ride-sourcing platforms to reduce cruising traffic. *Transportation Research Part C: Emerging Technologies*, 137:103562, 2022.
- [59] J MacGregor Smith. M/g/c/k blocking probability models and system performance. *Performance Evaluation*, 52(4):237–267, 2003.
- [60] Christian Dombacher. *Stationary queueing models with aspects of customer impatience and retrial behaviour*. PhD thesis, 2008.
- [61] ElectricRate. Cheap electricity rates in new york. <https://www.electricrate.com/residential-rates/new-york/>, 2022.

Appendix

Appendix A: Proof of Lemma 2

To prove Lemma 2, we first note that given δ , s , t_s , C , K , Q and V , P_V defined by (24j) and (26j) and t_w defined by (24k) and (26k) are monotonically increasing functions of γ due to the nature of M/M/Q/V queueing system and the mixed queueing system. Without loss of generality, we denote $P_V = \hat{P}_V(\gamma)$ and $t_w = \hat{t}_w(\gamma)$ defined by (24j) and (24k) under plug-in charging, and denote $P_V = \tilde{P}_V(\gamma)$ and $t_w = \tilde{t}_w(\gamma)$ defined by (26j) and (26k) under battery swapping. Below we show that in equilibrium (24), N_1 and N can be uniquely determined as a function of γ from (24d)-(24i), i.e., (i) of Lemma 2. The proof of (ii) is analogous and is thus omitted.

First, combining (24f), (24j) and (24i) derives N_2^m as a function of γ (denoted as $\hat{N}_2^m(\gamma)$):

$$\hat{N}_2^m(\gamma) = \frac{\gamma B}{\sqrt{K(1 - \hat{P}_V(\gamma))}}. \quad (36)$$

Substituting (36), (24g) and (24h) into (24e) further determines N_2 as a function of γ (denoted as $\hat{N}_2(\gamma)$):

$$\hat{N}_2(\gamma) = \frac{\gamma B}{\sqrt{K(1 - \hat{P}_V(\gamma))}} + \gamma \hat{t}_w(\gamma) + \gamma \hat{t}_s, \quad (37)$$

where $\hat{t}_s = \frac{(1-\delta)C}{s}$ is a constant. Besides, by (24l), we have:

$$N = \frac{\gamma(1-\delta)C}{l} + N_2^w + N_2^s. \quad (38)$$

Substituting (24g) and (24h) into (38) determines N as a function of γ (denoted as $\hat{N}(\gamma)$):

$$\hat{N}(\gamma) = \frac{\gamma(1-\delta)C}{l} + \gamma \hat{t}_w(\gamma) + \gamma \hat{t}_s. \quad (39)$$

Finally, subtracting (37) from (39) derives N_1 as a function of γ :

$$\hat{N}_1(\gamma) = \frac{\gamma(1-\delta)C}{l} - \frac{\gamma B}{\sqrt{K(1 - \hat{P}_V(\gamma))}}. \quad (40)$$

This completes the proof.

Appendix B: Proof of Lemma 3

Given δ , s , t_s , C , K , Q and V , note that $\hat{P}_V(\gamma)$ and $\tilde{P}_V(\gamma)$ monotonically increase with γ according to the nature of the queueing models. Besides, $\forall \gamma \geq 0$, $\hat{P}_V(\gamma) \geq 0$ and $\tilde{P}_V(\gamma) \geq 0$, and $\lim_{\gamma \rightarrow \infty} \hat{P}_V(\gamma) = 1$ and $\lim_{\gamma \rightarrow \infty} \tilde{P}_V(\gamma) = 1$. Below we show that if $K > \left(\frac{Bl}{(1-\delta)C}\right)^2$, there exist a unique $\hat{\gamma}_0 > 0$ and $\hat{\gamma}_* \in (0, \hat{\gamma}_0)$ such that $\hat{N}_1(\hat{\gamma}_0) = 0$, and $\forall \gamma \in (0, \hat{\gamma}_0)$, $\hat{N}_1(\gamma) > 0$ and $\hat{N}_1(\gamma) < \hat{N}_1(\hat{\gamma}_*)$, i.e., (i) of Lemma 3. The proof of (ii) is similar and is thus omitted.

We first rewrite $\hat{N}_1(\gamma)$ as:

$$\hat{N}_1(\gamma) = \gamma \left(\frac{(1-\delta)C}{l} - \frac{B}{\sqrt{K(1 - \hat{P}_V(\gamma))}} \right). \quad (41)$$

Let $\hat{B}(\gamma)$ be the term inside the bracket in (41), i.e., $\hat{B}(\gamma) = \frac{(1-\delta)C}{l} - \frac{B}{\sqrt{K(1-\hat{P}_V(\gamma))}}$. To guarantee the existence of positive $\hat{N}_1(\gamma)$, we need the maximum of $\hat{B}(\gamma)$ to be greater than zero, i.e., $\max_{\gamma \geq 0} \hat{B}(\gamma) > 0$. $\hat{B}(\gamma)$ is a decreasing function of γ since $\hat{P}_V(\gamma)$ monotonically increases with γ . The maximum of $\hat{B}(\gamma)$ is achieved at $\gamma = 0$. Therefore, it suffices to show that $\hat{B}(0) = \frac{(1-\delta)C}{l} - \frac{B}{\sqrt{K(1-\hat{P}_V(0))}} > 0$, which is equivalent to $K > \left(\frac{Bl}{(1-\delta)C}\right)^2$.

When $K > \left(\frac{Bl}{(1-\delta)C}\right)^2$, there exist $\gamma > 0$ such that $\hat{N}_1(\gamma) > 0$. Let $\hat{\gamma}_0 = \hat{B}^{-1}(0)$, where $\hat{B}^{-1}(\cdot)$ is the inverse function of $\hat{B}(\gamma)$. We have $\hat{N}_1(\gamma) > 0$ when $0 < \gamma < \hat{\gamma}_0$ due to the monotonicity of $\hat{B}(\gamma)$. Besides, since $\hat{N}_1(0) = 0$ and $\hat{N}_1(\hat{\gamma}_0) = 0$, by the continuity of $\hat{N}_1(\gamma)$, there must exist a $\hat{\gamma}_* \in (0, \hat{\gamma}_0)$ such that $\hat{N}_1(\hat{\gamma}_*) > \hat{N}_1(\gamma)$, $\forall \gamma \in (0, \hat{\gamma}_0)$. This completes the proof.

Appendix C: Proof of Proposition 1

To guarantee the existence of market equilibrium, we need to show that there exists strictly positive p_f , w^c , w^v , λ , γ , t_m , t_w , P_V , N , N_1 , N_2 , N_2^m , N_2^w , N_2^s satisfying (24) and (26), respectively. We have shown in Lemma 1 that there exists strictly positive w^c and w^v satisfying (24b)-(24c)/(26b)-(26c) if $N_1 \geq \left(\sqrt[3]{2} + \sqrt[3]{\frac{1}{4}}\right) (A\lambda)^{\frac{2}{3}} + \lambda\tau$, and $w^c = w^c(\lambda, N_1)$ and $w^v = w^v(\lambda, N_1)$ can uniquely derived from (24b)-(24c)/(26b)-(26c). Besides, we have shown in Lemma 2 that $P_V = \hat{P}_V(\gamma)$, $t_w = \hat{t}_w(\gamma)$, $N_1 = \hat{N}_1(\gamma)$, $N_2 = \hat{N}_2(\gamma)$, $N = \hat{N}(\gamma)$ can be derived from (24d)-(24l), and $P_V = \tilde{P}_V(\gamma)$, $t_w = \tilde{t}_w(\gamma)$, $N_1 = \tilde{N}_1(\gamma)$, $N_2 = \tilde{N}_2(\gamma)$, $N = \tilde{N}(\gamma)$ can be derived from (26d)-(26l), and $\hat{N}_1(\gamma) = \tilde{N}_1(\gamma)$. In this case, the market equilibrium (24) and (26) are equivalent to the following:

$$\left\{ \begin{array}{l} p_f = F_p^{-1} \left(\frac{\lambda}{\lambda_0} \right) - \alpha w^c \left(\lambda, \hat{N}_1(\gamma) \right) \quad (42a) \\ w^v = w^v \left(\lambda, \hat{N}_1(\gamma) \right) \quad (42b) \\ N = \frac{\gamma(1-\delta)C}{l} + \gamma \hat{t}_w(\gamma) + \gamma \hat{t}_s \quad (42c) \\ N_1 = \hat{N}_1(\gamma) = \frac{\gamma(1-\delta)C}{l} - \frac{\gamma B}{\sqrt{K(1-\hat{P}_V(\gamma))}} \quad (42d) \\ N_2 = \frac{\gamma B}{\sqrt{K(1-\hat{P}_V(\gamma))}} + \gamma \hat{t}_w(\gamma) + \gamma \hat{t}_s \quad (42e) \\ N_2^m = \frac{\gamma B}{\sqrt{K(1-\hat{P}_V(\gamma))}} \quad (42f) \\ N_2^w = \gamma \hat{t}_w(\gamma) \quad (42g) \\ N_2^s = \gamma \hat{t}_s \quad (42h) \\ P_V = \hat{P}_V(\gamma) \quad (42i) \\ t_w = \hat{t}_w(\gamma) \quad (42j) \\ \hat{N}_1(\gamma) \geq \left(\sqrt[3]{2} + \sqrt[3]{\frac{1}{4}} \right) (A\lambda)^{\frac{2}{3}} + \lambda\tau \quad (42k) \end{array} \right.$$

and

$$\left\{ \begin{array}{l} p_f = F_p^{-1} \left(\frac{\lambda}{\lambda_0} \right) - \alpha w^c \left(\lambda, \tilde{N}_1(\gamma) \right) \quad (43a) \\ w^v = w^v \left(\lambda, \tilde{N}_1(\gamma) \right) \quad (43b) \\ N = \frac{\gamma(1-\delta)C}{l} + \gamma \tilde{t}_w(\gamma) + \gamma \tilde{t}_s \quad (43c) \\ N_1 = \tilde{N}_1(\gamma) = \frac{\gamma(1-\delta)C}{l} - \frac{\gamma B}{\sqrt{K(1-\tilde{P}_V(\gamma))}} \quad (43d) \\ N_2 = \frac{\gamma B}{\sqrt{K(1-\tilde{P}_V(\gamma))}} + \gamma \tilde{t}_w(\gamma) + \gamma \tilde{t}_s \quad (43e) \\ N_2^m = \frac{\gamma B}{\sqrt{K(1-\tilde{P}_V(\gamma))}} \quad (43f) \\ N_2^w = \gamma \tilde{t}_w(\gamma) \quad (43g) \\ N_2^s = \gamma \tilde{t}_s \quad (43h) \\ P_V = \tilde{P}_V(\gamma) \quad (43i) \\ t_w = \tilde{t}_w(\gamma) \quad (43j) \\ \tilde{N}_1(\gamma) \geq \left(\sqrt[3]{2} + \sqrt[3]{\frac{1}{4}} \right) (A\lambda)^{\frac{2}{3}} + \lambda\tau \quad (43k) \end{array} \right.$$

where $F_p^{-1}(\cdot)$ is inverse function of $F_p(\cdot)$. For the profit maximization problem (23) and (25), we can equivalently treat λ and γ as decision variables/free variables. To prove Proposition 1, it is equivalent to show that there exists $\lambda \in (0, \lambda_0)$ and $\gamma \in (0, +\infty)$ such that

$$\left\{ \begin{array}{l} p_f = F_p^{-1} \left(\frac{\lambda}{\lambda_0} \right) - \alpha w^c \left(\lambda, \hat{N}_1(\gamma) \right) > 0 \quad (44a) \\ N_1 = \frac{\gamma(1-\delta)C}{l} - \frac{\gamma B}{\sqrt{K(1-\hat{P}_V(\gamma))}} > 0 \quad (44b) \\ N = \frac{\gamma(1-\delta)C}{l} + \gamma \hat{t}_w(\gamma) + \gamma \hat{t}_s > 0 \quad (44c) \\ N_2 = \frac{\gamma B}{\sqrt{K(1-\hat{P}_V(\gamma))}} + \gamma \hat{t}_w(\gamma) + \gamma \hat{t}_s > 0 \quad (44d) \\ N_2^m = \frac{\gamma B}{\sqrt{K(1-\hat{P}_V(\gamma))}} > 0 \quad (44e) \\ N_2^w = \gamma \hat{t}_w(\gamma) > 0 \quad (44f) \\ N_2^s = \gamma \hat{t}_s > 0 \quad (44g) \\ P_V = \hat{P}_V(\gamma) > 0 \quad (44h) \\ t_w = \hat{t}_w(\gamma) > 0 \quad (44i) \\ \frac{\gamma(1-\delta)C}{l} - \frac{\gamma B}{\sqrt{K(1-\hat{P}_V(\gamma))}} \geq \left(\sqrt[3]{2} + \sqrt[3]{\frac{1}{4}} \right) (A\lambda)^{\frac{2}{3}} + \lambda\tau \quad (44j) \end{array} \right.$$

and

$$\begin{cases}
p_f = F_p^{-1}\left(\frac{\lambda}{\lambda_0}\right) - \alpha w^c(\lambda, \tilde{N}_1(\gamma)) > 0 & (45a) \\
N_1 = \frac{\gamma(1-\delta)C}{l} - \frac{\gamma B}{\sqrt{K(1-\tilde{P}_V(\gamma))}} > 0 & (45b) \\
N = \frac{\gamma(1-\delta)C}{l} + \gamma \tilde{t}_w(\gamma) + \gamma \tilde{t}_s > 0 & (45c) \\
N_2 = \frac{\gamma B}{\sqrt{K(1-\tilde{P}_V(\gamma))}} + \gamma \tilde{t}_w(\gamma) + \gamma \tilde{t}_s > 0 & (45d) \\
N_2^m = \frac{\gamma B}{\sqrt{K(1-\tilde{P}_V(\gamma))}} > 0 & (45e) \\
N_2^w = \gamma \tilde{t}_w(\gamma) > 0 & (45f) \\
N_2^s = \gamma \tilde{t}_s > 0 & (45g) \\
P_V = \tilde{P}_V(\gamma) > 0, t_w = \tilde{t}_w(\gamma) > 0 & (45h) \\
\frac{\gamma(1-\delta)C}{l} - \frac{\gamma B}{\sqrt{K(1-\tilde{P}_V(\gamma))}} \geq \left(\sqrt[3]{2} + \sqrt[3]{\frac{1}{4}}\right) (A\lambda)^{\frac{2}{3}} + \lambda\tau & (45i)
\end{cases}$$

Note that (44) and (45) have the same form. Below we show the existence of market equilibrium (24) by justifying (44), i.e., (i) of Proposition 1. The proof of (ii) is analogous and is thereby omitted.

First, the positivity of P_V and t_w , i.e., condition (44h) and (44i) is naturally satisfied due to the nature of queueing models. Further, it is obvious that $N, N_2, N_2^m, N_2^w, N_2^s > 0$, i.e., conditions (44c)-(44g) given $t_w > 0$ and $P_V \in [0, 1)$. Therefore, $\forall \gamma \in (0, \infty)$, $N, N_2, N_2^m, N_2^w, N_2^s, t_w > 0$, i.e., conditions (44c)-(44i).

Next, we show that there exists $\gamma > 0$ such that $N_1 > 0$, i.e., condition (44b). Based on the result of Lemma (3), $\hat{N}_1(\gamma) > 0$ when $\gamma \in (0, \hat{\gamma}_0)$.

Next, we show that there exists $\gamma \in (0, \hat{\gamma}_0)$ and $\lambda \in (0, \lambda_0)$, such that $\frac{\gamma(1-\delta)C}{l} - \frac{\gamma B}{\sqrt{K(1-\tilde{P}_V(\gamma))}} \geq \left(\sqrt[3]{2} + \sqrt[3]{\frac{1}{4}}\right) (A\lambda)^{\frac{2}{3}} + \lambda\tau$, i.e., condition (44j). Note that the LHS of (44j) is $\hat{N}_1(\gamma) = \frac{\gamma(1-\delta)C}{l} - \frac{\gamma B}{\sqrt{K(1-\tilde{P}_V(\gamma))}}$. Based on the result of Lemma 3, it initially increases with γ and then decreases within $(0, \hat{\gamma}_0)$, and the the maximum of $\hat{N}_1(\gamma)$ is achieved at $\hat{\gamma}_*$. The RHS of (44j) is a continuous and strictly increasing function of λ . By continuity, there must exist $0 < \gamma_1 < \hat{\gamma}_* < \gamma_2 < \hat{\gamma}_0$ and $0 < \lambda_1 < \lambda_0$ such that $\hat{N}_1(\gamma) \geq \left(\sqrt[3]{2} + \sqrt[3]{\frac{1}{4}}\right) (A\lambda)^{\frac{2}{3}} + \lambda\tau$ when $\gamma \in (\gamma_1, \gamma_2)$ and $\lambda \in (0, \lambda_1)$.

Next, we show that there exists $\gamma \in (\gamma_1, \gamma_2)$ and $\lambda \in (0, \lambda_1)$ such that $p_f > 0$, i.e., condition (44a). Note that $w^c(\lambda, N_1)$ is derived from (24b)-(24c). Substituting (24c) into (24b), we have:

$$w^c = \frac{A}{\sqrt{N_1 - \lambda\mu - \lambda w^c}}. \quad (46)$$

Plugging (46) into (44a) leads to:

$$p_f = F_p^{-1}\left(\frac{\lambda}{\lambda_0}\right) - \frac{\alpha A}{\sqrt{N_1 - \lambda\tau - \lambda w^c}}. \quad (47)$$

By assumption, $F_p(\cdot)$ is a strictly decreasing function, thus $F_p^{-1}\left(\frac{\lambda}{\lambda_0}\right)$ monotonically decreases with λ . Therefore, p_f is a decreasing function with respect to λ and an increasing function with respect to N_1 . The

maximum of p_f is

$$p_f^{\max} = \lim_{\lambda \rightarrow 0} F_p^{-1} \left(\frac{\lambda}{\lambda_0} \right) - \frac{\alpha A}{\sqrt{N_1^{\max}} - \lambda \tau - \lambda w^c} = F_p^{-1}(0) - \frac{\alpha A}{\sqrt{N_1^{\max}}}, \quad (48)$$

where N_1^{\max} is the maximum of N_1 . Based on the result of Lemma 3, the maximum of $\hat{N}_1(\gamma)$ is $\hat{N}_1^{\max} = \hat{N}_1(\hat{\gamma}_*)$. To guarantee the existence of positive p_f , we need that

$$p_f^{\max} = F_p^{-1}(0) - \frac{\alpha A}{\sqrt{\hat{N}_1^{\max}}} > 0, \quad (49)$$

which is equivalent to $F_p \left(\frac{\alpha A}{\sqrt{\hat{N}_1^{\max}}} \right) > 0$. Under this assumption, there must exist $0 < \lambda_2 < \lambda_1$ and $(\gamma_3, \gamma_4) \subset (\gamma_1, \gamma_2)$ such that $p_f > 0$ when $\lambda \in (0, \lambda_2)$ and $\gamma \in (\gamma_3, \gamma_4)$.

Finally, we take the intersection of all the derived conditions to show the feasibility of (44). Given the assumptions that $K > \left(\frac{Bl}{(1-\delta)C} \right)^2$ and $F_p \left(\frac{\alpha A}{\sqrt{\hat{N}_1^{\max}}} \right) > 0$, (44) hold when $\lambda \in (0, \lambda_2)$ and $\gamma \in (\gamma_3, \gamma_4)$. This completes the proof.

Appendix D: Calibration of model parameters A and B

Both the passenger waiting time function (3) and the vehicle searching time function (9) follow the same 'square root law'. Here we calibrate the model parameters of the vehicle searching time function (9) based on realistic geographic and traffic data of New York City to determine the value of the parameter B . The calibration of the passenger waiting time function (3) follows the same approach, and the value of parameter A is taken to be the same as that of B .

Consider the numerical simulation for New York City, where a fleet of vehicles and a number of charging/battery swapping stations are randomly generated and uniformly distributed across the city. We assume that vehicles travel to the nearest charging/battery swapping stations for energy top-up and calculate the average travel time to the charging/battery swapping stations. We vary the number of charging/battery swapping stations and calculate vehicles' average travel time to charging/battery swapping stations. The scatter plots in Figure 9 show the calculated average travel time under different supplies of charging infrastructures, which graphically indicates that the vehicle searching time follows the 'square root law'. Therefore, we fit the vehicle searching time function (9) based on the simulation data and calibrate that $B = 230$. The solid line in Figure 9 shows the fitted vehicle searching time function $t_m = \frac{230}{\sqrt{K}}$ with $R^2 = 0.9943$. It indicates that the proposed searching time function (9) is a good fit for the vehicle searching time for charging under the nearest-neighbor matching.

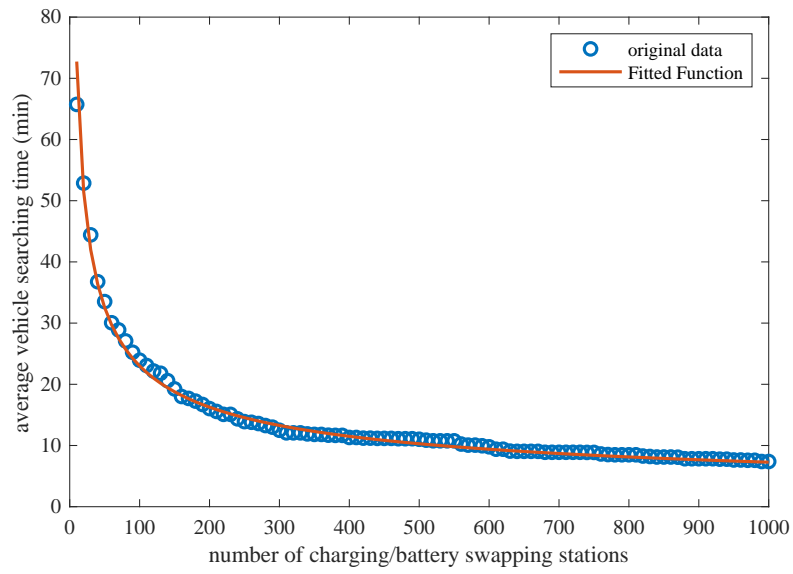


Figure 9: (1) scatter plots: simulated average vehicle searching time under distinct supplies of charging/battery swapping stations; (2) solid line: fitted vehicle searching time function $t_m = \frac{230}{\sqrt{K}}$ with $R^2 = 0.9943$.